

1 **Coastal erosion in NW Spain: recent patterns under extreme storm wave events**

2 G. Flor-Blanco¹, J. Alcántara-Carrió^{2,3}, D.W.T. Jackson^{4,5}, G. Flor¹, C. Flores-Soriano¹

3 1. Department of Geology, C/ Arias de Velasco, s/n. 33005 Oviedo, Universidad de
4 Oviedo, Spain UNESCO PICG Group 639. gfb@geol.uniovi.es; gflor@geol.uniovi.es;
5 c.flores.soriano@gmail.com

6 2. Department of Geosciences, Universidade de Aveiro, 3810-193 Aveiro, Portugal.
7 javier.alcantara@ua.pt

8 3. Department of Geology and Geochemistry, Universidad Autónoma de Madrid, Madrid,
9 Spain.

10 4. Centre for Coastal and Marine Research, School of Geography and Environmental
11 Sciences, Ulster University, Northern Ireland, UK. d.jackson@ulster.ac.uk

12 5. Geological Sciences, University of KwaZulu-Natal, South Africa

13 **ABSTRACT**

14 Coastal dunes are sensitive to both anthropic and natural processes of erosion. In this
15 study, we analyse the geomorphic changes in 15 dune-fringed coastlines of Asturias
16 (NW Spain) for the period 1992 to 2014 to determine specific drivers of erosion. Coastline
17 migration patterns were obtained using geospatial analysis of vertical aerial images and
18 field surveys. The annual and maximum wave energy, maximum significant wave height,
19 duration and number of storm events were determined for each climatic year by using
20 available wave data from both recorded buoy data (1997-2014) and the WAM numerical
21 model (1956-2015). The study shows that since 2006, coastline retreat has significantly
22 accelerated along the Asturias coast. In particular, severe erosion of sandy beaches and
23 dunes occurred in 2013/14, reaching up to 40 m of coastline retreat and destroying
24 numerous ports and seafront promenades. Increased frequency of unusually strong
25 storm waves, with significant wave height (H_s) exceeding 9 m, together with an unusual
26 5° westward variation from the mode in offshore wave approach direction during these
27 storms, appear to be the main catalysts in heightened erosion capacity of storm waves

28 in the 2013/14 period. This resulted in the removal of small dune areas and a severe
29 recession in the easternmost part of the largest (natural) dune fields in the region. Under
30 these stormy periods, foredunes and climbing dunes developed notably pronounced
31 escarpments and blowouts, with sand subsequently relocated into the foreshore and
32 backshore zones. This study demonstrated that increased frequency in powerful storm
33 events ($H_s > 9$ m) and an alteration in storm approach direction, can lead to significantly
34 enhanced erosion of dune coastlines, even along those that are modally-attuned to high
35 energy events.

36 **Keywords:** coastal dunes, coastline retreat, climate change, storm frequency, storm
37 approach angle.

38

39 1- INTRODUCTION

40 Morphological changes in the coastal zone are the result of complex interactions
41 between natural and anthropogenic processes, operating over various spatial and
42 temporal scales (Ruggiero et al., 2005; Crapoulet et al., 2015, Jackson and Short, 2020,
43 Short and Jackson, 2021). These processes can act within short (event) time scales,
44 such as storm wave events (Castelle and Harley, 2020), or longer cyclical periods, such
45 as tidal forcing, seasonal variations in wave climate (Senechal and Ruiz de Alegría-
46 Arzaburub, 2020), and inter-annual to decadal-scale variations in the ocean-atmosphere
47 system (Nordstrom, 1980; Aubrey and Ross, 1985; Zoulas, 2008; Yates et al., 2009b).
48 They can also exist over even longer timelines as with Relative Sea Levels (Trindade
49 and Ramos-Pereira, 2013).

50 Over short time-scales, beach morphodynamics are typically controlled through
51 seasonal weather patterns (Fontán-Bouzas et al., 2009; 2019; Senechal and Ruiz de
52 Alegría-Arzaburub, 2020). In these scenarios, a close relationship usually exists between
53 morpho-sedimentary changes and the energy of the incident waves, with storm waves

54 normally inducing rapid coastal erosion, while beach rebuilding during calm weather is
55 much slower (Davis and Fox, 1972; Wright and Short, 1984, Castelle and Harley, 2020).
56 Storm waves can also exhibit pseudo-cyclical patterns of change over shorter intervals,
57 varying from a few days to over several weeks (Nordstrom, 1980).

58 Sandy beaches can be particularly vulnerable to storm wave events (Fenster et al., 2001;
59 Fontán-Bouzas et al., 2009; Cid et al., 2016, Castelle and Harley, 2020) and many
60 studies have attempted to model the impact of coastal storm events, with a focus largely
61 on the response of sand beaches to storms (Lee et al., 1998; Dail et al., 2000; Hill et al.,
62 2004; Cooper et al., 2004; Von Storch and Woth, 2008; Yates et al., 2009a, Guisado-
63 Pintado and Jackson, 2018; 2019, Anfuso et al. 2020). Within the embayed Asturian
64 coast (NW Spain), sediment supply is not provided from longshore drift sources, and
65 instead largely originates from local riverine sources (Fig.1).

66 **INSERT FIGURE 1**

67 Coastal dunes play a key role in stabilising the coast, acting as an essential sedimentary
68 reserve for beaches, particularly during intense storms and very high tides. Dunes are
69 therefore an important source of sediments with which to regenerate beaches from
70 (Hesp, 2002, 2011; Hesp and Smyth, 2016). The sedimentary thickness of coastal dunes
71 is strongly related to sand availability on beaches (Fontán Bouzas et al., 2013) and the
72 evolution of beaches and dunes is therefore strongly inter-related (Short and Hesp, 1982;
73 Hesp, 2011), with dune behaviour directly forced by storm wave events.

74 Human activities also modify the evolution of coastal areas (Alonso et al., 2002;
75 Augustinus, 2003), often triggering significant changes (Rodríguez-Ramírez et al., 2008;
76 Flor-Blanco et al., 2015a; Flor et al., 2015, Hernández-Cordero et al., 2018), which
77 ultimately affect coastal retreat dynamics (Ruz et al., 2005). The Intergovernmental
78 Panel on Climate Change (IPCC) predicts that climate change will magnify extreme
79 events (Church et al., 2013). Vousdoukas et al. (2015) have shown the interaction

80 between storm surge levels and the increases in relative sea level, while Plomaritis et al.
81 (2015) purport that large-scale atmospheric phenomena are the main cause of diversity
82 in recent storm patterns.

83 Sea-level also plays an important role in promoting the retreat of most of the world's
84 shorelines, particularly along dune-fringed coasts (Carter et al., 1990, Carter, 1991).
85 Between 1961 and 2008, secular sea level rose by 1.8 ± 0.4 mm yr⁻¹, and is expected to
86 continue to rise (0.5 to 1.0 m) until 2100 and beyond (Church et al., 2013). The global
87 trend published by IPCC (2014) shows projected rates of around 3.2 and 3.4 ± 0.4 mm
88 y⁻¹ and Vousdoukas et al (2017) reinforced this idea which consider that future extreme
89 levels along Europe's coastlines is on average projected to increase by 57 cm, taking
90 into account to the changes in storm surges and waves enhance the effects of relative
91 sea level rise along the majority of northern European coasts and lees in the south.
92 Moreover, different effects of climate change, such as the global sea level rise and the
93 changes in the regional storm climate and the atmospheric circulation patterns are
94 expected to increase in the future in the Spanish coast (Rasilla et al., 2018)

95 Exceptionally intense storm wave events in recent years have increased awareness of
96 the frequency, impact, and roles of storms in the European Union (Cooper et al., 2004;
97 Ciavola et al., 2011; Rangel-Buitrago and Anfuso, 2013; Loureiro et al., 2014; Guisado-
98 Pintado and Jackson, 2018; 2019; Anfuso et al., 2020), the barrier islands of the Eastern
99 United States (US) (Anthony, 2013), and in East Asia (An et al, 2018).

100 Strong winter storms in February and March 2014 adversely affected European Atlantic
101 shorelines, causing significant impacts on economies, society and the environment, with
102 recent research on this focusing mostly on the north Atlantic coast (Carretero et al., 1998;
103 Goldenberg et al., 2001; Komar and Allan, 2008; Chaaban et al., 2012; Rangel-Buitrago
104 et al., 2016; Masselink et al., 2016; Castelle et al., 2017), and on the Iberian Peninsula

105 (Rasilla et al., 2014; Flor et al., 2014; Plomaritis, et al., 2015; Cid et al., 2015; Flor et al.,
106 2019).

107 The current study analyses the geomorphological evolution of 15 dune-fringed coastal
108 stretches of Asturias between 1992 and 2014 (Fig. 1), and the relationship between this
109 evolution and the regional storm wave pattern. The work centres on the exceptionally
110 large storm waves of the 2013/14 climatic year, in order to examine the severe erosion
111 patterns that resulted.

112 **2- REGIONAL SETTING**

113 The Asturian coast, located on the NW Iberian Peninsula, is a mostly cliff-type coast. Its
114 geomorphologic evolution is controlled by both the lithology and its structural
115 arrangement, with a general West to East alignment, although various sections are
116 oriented NW-SE and NE-SW (Flor and Flor-Blanco, 2014a). The coastal hinterland has
117 a relatively smooth relief due to several old erosive flat surfaces that are positioned at
118 various heights (Flor and Flor-Blanco, 2014a; Domínguez-Cuesta et al., 2015, López-
119 Fernández et al., 2020). In addition, it is one of the most natural coasts of the Iberian
120 Peninsula and has been afforded several conservation protections including Sites of
121 Community Interest (SCI), as well as many wetlands and estuaries classed as Special
122 Protection Areas (SPA).

123 The most frequent wave approach directions on the inner continental shelf are from the
124 first and fourth quadrants, with waves coming from the NE in fair weather and waves
125 from the NW during storm events. Offshore significant height (H_s) is usually greater than
126 1.7 m, with the highest H_s recorded at the Peñas buoy since 1998 being 23.3 m (Flor et
127 al., 2014a). The tides affecting the Cantabrian coast (Bay of Biscay) are semi-diurnal,
128 and average ranges are generally meso-tidal (2-4m) for 68.52% of the year.

129 Sandy, embayed beaches are prevalent, with their siliciclastic sediments originating from
130 the mountain and lowland coastal rivers, but bioclastic carbonate fractions also appear

131 in many coastal sectors (Flor et al., 1982). Many Asturian beaches are sheltered and
132 generally protected from the NW waves, such as those-generated east of Peñas Cape
133 (Flor, 1978) or locally bounded by large headlands and high cliffs slopes.

134 Sandy beaches with abundant sand sources have formed large dune fields close to wide
135 estuaries or those linked to the eastern side of the mouths of the major (Eo, Navia, Nalón,
136 and Sella) and minor (Aboño, Piles, Linares, Libardón, and Espasa) river systems (Fig.
137 1; Flor and Flor-Blanco, 2014b). The orientation of the dunes is associated with the NW
138 and NE prevailing wind directions, although the SW winds are dominant (Flor and Flor-
139 Blanco, 2014b).

140 **3- METHODOLOGY**

141 **3.1. Wave data analysis**

142 The local wave regime data was derived from both offshore buoys and the WAM
143 numerical prediction model (Puertos del Estado. Government of Spain). Wave data from
144 Estaca de Bares (44.12°N, 7.67°W; 1800 m water-column depth, 41 kilometres from the
145 coast, 01/01/1996 to 02/02/2015) and Cabo de Peñas (43.75°N, 6.16°W, 615 m water-
146 column depth, 20 kilometres from the coast, 06/09/1997 to 30/01/2015) buoys
147 (Deepwater Buoy Network) were examined (Fig 1). These wave data were initially
148 recorded in 3-hours intervals, but have been recorded in 1-hour intervals since January
149 1998. Secondly, the wave database (1958-2015) from the offshore 1052075 SIMAR
150 point was obtained by the WAM wave prediction model in 1-hour intervals. Significant
151 wave height (H_s), maximum wave height (H_{max}), peak period (T_p) and wave approach
152 direction were considered from both wave databases. Additionally, for 2014, tidal records
153 from Musel Port (Gijón) and wave records from a buoy located at Cudillero (43.60°N,
154 6.13°W) were also obtained.

155 The beginning of a storm event was considered when offshore H_s overtopped 3 m and
156 its duration determined by the successive hours over this critical value. Based in the Airy

157 Theory, the total energy (J m⁻²) for each storm event was determined after the n
158 successive H_{s0} (m) values during the event, and in consideration of the number of waves
159 that occurred each hour after the T_p (s). This is expressed in the following equation:

$$160 \quad E_T = \frac{1}{2} \rho g \sum_{i=0}^n H_{s_{0i}}^2 \left(\frac{60}{T_{pi}} \right) \quad (1)$$

161 Where E_T is the total energy of the storm event, ρ is seawater density, g is gravity
162 acceleration, H_{si} is the offshore significant wave height for the i hour, with a total duration
163 of the storm event of n hours, and T_{pi} is the associated peak period for the hour i.

164 Sea state curves were plotted for each buoy, but statistical analyses of these data series
165 were not used because they contained too many gaps. In contrast, the wave database
166 obtained from the numerical model allowed the determination of seven parameters for
167 each climatic year (beginning July 1st and ending the following June 30th): i) maximum
168 H_s; ii) maximum energy of a storm event; iii) number of storm events; iv) total duration of
169 the storm events; v) maximum duration of a storm event; vi) average duration of storm
170 events; and vii) total annual energy. Finally, directional histograms were plotted using
171 Grapher of Golden Software Package for all storm wave events (H_s>3m) and only for
172 extreme storm wave events (H_s>7m), considering both the entire study period (1958-
173 2015) and only the climatic year 2013-2014.

174 **3.2. Coastline evolution pattern**

175 The recent coastline evolution patterns (1992 to 2014) of 15 dune fields in the Asturian
176 coast (Fig. 1) were assessed through the analysis of vertical aerial images (1992 and
177 2001), ortho-photographs (2006, 2009, 2011 and 2014) and field measurements in
178 Spring 2015.

179 Google Earth and Bing Maps images were used for reviewing satellite photographs. The
180 images were included in a Geographic Information System (GIS) and georeferenced by
181 rectification with a rubber-sheeting process using checkpoints on vector topographic

182 maps with the ArcGIS (ESRI) software tools. To calculate RMS error, each image was
183 independently georeferenced based on the 2014 orthophoto mosaic and ground control
184 points derived from buildings and parcel boundaries. The RMS error achieved was less
185 than 0.5 m.

186 Recent frontal limits of all dune fields were measured during the spring and summer of
187 2014 using a Leica Disto D5 laser distance meter and a GPS to validate the progradation
188 or erosion rates from contemporaneous orthophotographs and to assess the effects of
189 the exceptionally strong storm waves of February and March 2014.

190 Finally, the effects of storm waves in the geomorphological evolution of the Asturian
191 coastal dune over a period of more than two decades were obtained by combining the
192 analysis of the shoreline changes with corresponding wave patterns. For this analysis,
193 net seaward advance and landward retreat of the frontal dune line were calculated by
194 considering three cross-shore profiles for each dune field (WP= Western profile, CP=
195 Central profile, EP= Eastern profile), by comparing aerial photographs/orthophotographs
196 and field measurements since the last decade of the 20th century with field
197 measurements during 2014. All profiles were selected from locations where information
198 on their historical evolution was known, avoiding heavily modified/managed areas.

199 **4. RESULTS**

200 **4.1. Wave and tidal forcings**

201 The wave databases recorded by the Estaca de Bares and Cabo de Peñas buoys (Fig.
202 1) show that the winter of 2013-2014 had the highest number of extreme storm wave
203 events ($H_s > 7\text{m}$) of the entire 22-year study period, although some small differences
204 between both wave records were observed (Fig. 1, supplementary material).
205 Nevertheless, the data series presented gaps of 30.99% and 17.37% at Estaca de Bares
206 and Cabo Peñas, respectively. Therefore, results from these buoys were considered
207 unreliable.

208 The analysis of the wave database from the WAM model, without gaps, shows that
209 compared with previous decades, the period 2000-2005 corresponded to a low energy
210 phase. Subsequently, since 2006, storm wave events again became more energetic and
211 recurrent (Fig. 2).

212 **INSERT FIGURE 2**

213

214 A window of low energy was identified in the period 2000-2005, particularly for the
215 climatic year 2004-2005, with a decrease in the total number of storm events, total
216 duration, maximum duration, total annual energy and maximum energy of the storms.
217 These fair weather conditions were in consonance with storm conditions in previous
218 decades, and since 2006 storm energy increased again (Fig. 2; Fig. 1, supplementary
219 material).

220 The wave database from the WAM model also confirms that the period 2013-2014 was
221 particularly energetic. However, it was not overly different to some previous years for
222 some parameters. Thus, considering all storm wave events ($H_s > 3\text{m}$), similar values of
223 total annual energy occurred in 1959-1960, 1976-77, and 1994-95, and the total annual
224 energy was clearly highest in the years 1960-1961, 1971-72, 1977-78, 1982-83, 1983-
225 84, and 1993-94. 2013-14 did not represent a year with the strongest storm event nor
226 the maximum H_s . The average energy was not any higher in this year in comparison to
227 other years, and neither the average duration of storms and maximum duration of a storm
228 was especially higher compared to all other years in the study period (Fig. 2).

229 Considering the storm frequency after H_s intervals however, it can be observed that
230 2013/14 had an unusual abundance of storm waves with a $H_s > 9\text{ m}$, only surpassed by
231 1982/83 (Table 1). Therefore, 2013/14 was in the top 5% of all years recorded after the
232 occurrence of extreme storm waves ($H_s > 9\text{ m}$), i.e. the key to the erosional power of

233 2013/2014 was not the occurrence of storm events with $H_s > 3m$, but the high number of
 234 *extreme* storm events with $H_s > 9 m$.

235

Range of Hs (m)	1958-2015	1960-1961	1971-1972	1977-1978	1982-1983	1983-1984	1993-1994	1994-1995	2013-2014
3.1-4.9	81.14	84.01	78.52	71.49	80.13	70.43	77.99	74.76	81.94
5.0-6.9	15.25	14.80	17.15	21.19	14.98	26.18	19.23	22.39	15.65
7.0-8.9	3.22	1.12	3.97	7.33	3.94	3.20	2.78	2.85	1.91
9.0-10.9	0.35	0	0.36	0	0.79	0.19	0	0	0.50
11.0-12.9	0.04	0	0	0	0.15	0	0	0	0

236

237 **Table 1.** Percentage distribution of storm wave events obtained from the WAM numerical model
 238 for the whole period (1st July 1958 - 30th June 2015), and for the nine climatic years with highest
 239 total annual energy.

240

241 Another noteworthy observation is that the typical wave approach direction for storm
 242 events was on most occasions from the north-west for the entire study period, however
 243 during 2013/14, a small change (5° westward from the mode) occurred. This change in
 244 wave approach direction is much more evident only during extreme storm waves (Fig.
 245 3). Buoy data also picks up this directional change in wave approach angle, previously
 246 undetected for this period. This change in offshore approach direction under storm wave
 247 scenarios implicates variations in the wave propagation patterns and incidence angle as
 248 being more impactful for coastal dune-beach systems.

249

INSERT FIGURE 3

250 The storm surges (meteorological tides), associated with low atmospheric pressure
 251 systems and astronomical tides had an adversely effect, increasing the destructive effect
 252 of storm waves. Indeed, the storm wave events on February 1-2 and March 3-4, when

253 the State Port buoys detected $H_s > 11\text{m}$, coincided with high spring tides, reaching up to
 254 4.61 m of tidal range (Table 2).

255 The recurrence of this type of strong storms over the last 20 years is remarkable, as
 256 between 1998 and 2015 there have been up to 36 storm events of $H_s > 7\text{m}$, while between
 257 1956 and 1998 there were only 2 (Source: Buoys-Puertos del estado. Ministerio de
 258 Fomento). This trend has continued until 2020.

259

CABO PEÑAS BUOY (43.75°N, 6.17°W)	
01-02/02/2014	03-04/03/2014
MAXIMUM HEIGHT (m)	
11.3	11.7

260

01-02/02/2014			
HIGH TIDES		LOW TIDES	
(h/m)	(h/m)	(h/m)	(h/m)
04:58/4.79	17:22/4.40	11:07/0.18	23:34/0.33
RANGE: 4.61 m		RANGE: 4.07 m	

261

02-03/03/2014			
HIGH TIDES		LOW TIDES	
(h/m)	(h/m)	(h/m)	(h/m)
04:38/4.70	16:58/4.40	10:44/0.15	23:02/0.24
RANGE: 4.55 m		RANGE: 4.16 m	

262

263 **Table 2.** Maximum significant height (m) recorded in Cape Peñas buoy and tidal ranges (m)
 264 recorded in Musel Port (Source: Puertos del estado. Ministerio de Fomento).

265

266 **4.2. Dune coastline evolution**

267 The Asturian dune fields are characterised by having formed between rocky
268 promontories on a cliffed coast. According to Flor et al. (2011), the predominant
269 morphologies are sand-sheet, climbing, tongue-like, with the most extensive being those
270 associated with estuary spit barriers (Quebrantos, Salinas, Rodiles and Vega) or
271 adjacent to estuary mouths such as Xagó (Fig. 4). In the latter, significant foredune
272 morphologies are clearly evident. In all of the dune coastlines examined, five have been
273 previously altered through anthropogenic activities (jetties or partial occupation), mining
274 activity, and in some cases, dredging and dumping from ports. All other stretches are
275 smaller, except for Vega, and represent natural sites (Fig. 4).

276 **INSERT FIGURE 4**

277

278 **4.2.1. Shoreline behaviour and dune area changes at human impacted sites**

279 In the case of Navia, between 1992 and 2011, during the last decade of the 20th century,
280 dunes were eroded on their western (-3.56 m) and eastern sides (-8.26 m). Shoreline
281 recovery between 2001 and 2006 had rates of 0.70 m yr⁻¹ (3.52 m) in West Profile (WP),
282 1.28 m yr⁻¹ (6.39 m) in Central Profile (CP), and 1.57 m yr⁻¹ (7.86 m) in East Profile (EP).
283 Since this year, recession was common throughout the dune front until the winter storms
284 of 2014. In 2009, changes were observed in dune front position with recessions of -0.95
285 m in the west and -0.10 m in the east; nevertheless, the central parts of the dunes
286 prograded (1.41 m). Recession rates between 2011 and 2014 were -1.56 m yr⁻¹ in WP
287 and with a maximum of -0.59 m yr⁻¹ in CP and EP (Figs. 4 and 5), with a general surface
288 loss of 1,194 m² (Fig. 5; Table I, supplementary material).

289

INSERT FIGURE 5

290 Similarly, the Quebrantos dune field is part of the confining barrier of the Nalón estuary.
291 Between 1992 and 2001, the system prograded (1 m yr⁻¹ in WP, 1.52 m yr⁻¹ in CP, and
292 1.91 m yr⁻¹ in EP), but the surface was reduced at the end of the 1990s due to the removal
293 of the eastern sector by the construction of a car park (Flor-Blanco et al., 2015a). The

294 continued progradation occurred until 2006, but to a lesser extent (Fig. 4 and 5; Table I,
295 supplementary material). Since then, recession began with rates of around -0.90 m yr^{-1}
296 (-2.71 m) until 2009 (Table I, supplementary material). In the next photograph (2011),
297 the dune front retreated -3.0 m yr^{-1} (CP), -1.21 m (EP), and recovered 0.38 m (WP).
298 Therefore, in last strongest storms in 2014, the recession was higher than it was in 2011,
299 mainly in the western region with between -16 m and approximately -11 m on the rest of
300 the dune front (Fig. 4 and 5; Table I, supplementary material).

301 Salinas-El Espartal dune field has been eroding since the 1970s and became more
302 pronounced in the 1990s and in 2014 due to surge events (Fig. 6). The calculated
303 recession for the period 1992 to 2014 is 32.20 m (-1.43 m yr^{-1}) in the western part, 31.57
304 m (1.43 m yr^{-1}) in central areas, and 10.23 m (-0.46 m yr^{-1}) in the east, with an estimated
305 loss of $121,404.65 \text{ m}^2$ surface area (Table I, supplementary material). This was caused
306 by the growing human occupation and the retreat of the dunes' front (Fig. 4).

307 Up until 2014, some parts of the Salinas-El Espartal dune field, like in other systems,
308 showed averaged erosion values of 20 m (-1.05 m yr^{-1})(WP), 18.56 m (-0.97 m yr^{-1}) (CP),
309 and 19 m (-0.32 m yr^{-1}) (EP) (Figs. 4 and 5; Table I, supplementary material). However,
310 the storms of 2014 caused clear erosion of the coastline, less in the eastern sector as a
311 result of sedimentary accumulation due to beach drift in this direction. Results show a
312 maximum recession of -12.20 m in WP, -13.01 m in CP, and -4.03 m in EP (Figs. 4 and
313 5; Table I, supplementary material). This dune field was one of the most impacted by this
314 event, including the west jetty of the Avilés Estuary mouth and the seafront promenade
315 of Salinas (Flor et al., 2013).

316 The Xagó system has on the other hand prograded since the 1980s, with intervening
317 short erosive periods (Figs. 4, 5 and 6), some of which are visible in the rest of the
318 Asturian coast dune systems, with a surface area increase of $1,628.43 \text{ m}^2 \text{ yr}^{-1}$ since the
319 1980s through to 2006, when it reached its maximum extent of $455,120 \text{ m}^2$ (Figs. 4 and

320 5; Fig. I, supplementary material). This was mainly due to discharges of dredged material
321 from the Avilés estuary. This increase was more significant in the central and eastern
322 parts, with 39.46 m (1.72 m yr^{-1}) recorded in CP and 36.64 m (1.6 m yr^{-1}) in EP, while in
323 WP, rates were only 8.12 m (0.35 m yr^{-1}) (Table I, supplementary material). It is worth
324 noting that, despite contributions from sediment dredging, dunes are currently
325 experiencing an erosive period in the western and central areas (Flor-Blanco et al.,
326 2013). Between 2006 and 2009, the western and central fringes decreased 12.48 m (-
327 4.16 m yr^{-1}) and 4.70 m (-1.57 m yr^{-1}), respectively; but since 2009, the foredune in
328 general recovered, although it receded 2.27 m specifically in the western part (Figs. 4
329 and 5; Table I, supplementary material). Since 2011, the seaward most foredune has
330 been decreasing substantially (Figs. 5 and 6).

331 The storms during the winter of 2014 resulted in significant foredune erosion in all sites,
332 with a maximum of -6.48 m in the western area, a minimum of -2.91 m in the eastern
333 sector, and similar amounts in the central part of the foredune (Figs. 4 and 5; Table I,
334 supplementary material). Small tabular dune in the easternmost has disappeared and
335 the upper beach, like the other studied dune fields, also lost sand, inducing a scarped
336 dune frontage.

337 Rodiles dune field (Villaviciosa estuary, Fig. 4), up until 2001, showed a recession of -
338 2.78 m in WP (-0.40 m yr^{-1}), -7.41 m in CP (-1.06 m yr^{-1}), and 9.89 m in EP (1.41 m yr^{-1}).
339 Between 2000 and 2011, the dune surface increased 14,145.11 m^2 ($1,414.51 \text{ m}^2 \text{ yr}^{-1}$)
340 with a recovery of sand area to an extent similar to 1970 (Flor-Blanco et al., 2015a) which
341 was probably helped by management intervention restricting access (Flor et al., 2015).
342 However, the erosion trends began to change since 2011, especially in the winter of
343 2014, when the recession was focused in the foredune of EP (-14.54 m) and to a lesser
344 extent in WP (-0.93 m) and CP (-0.78 m) (Figs. 4 and 5; Table I, supplementary material).

345 In general, the dune recession in these dune fields has been contrasted with the
346 reduction of their surface, already undermined by the anthropic occupation (Fig. 6)

347

INSERT FIGURE 6

348 **4.2.2. Shoreline behaviour and dune area changes at natural sites**

349 The 1990s was a significant erosive period in most natural dune systems and in other
350 similar cases outlined below (Fig. 4 and 7; Table II, supplementary material). Barayo
351 presents the most erosion, with a decrease of 6,742 m² (749.21 m yr⁻¹). However, the
352 Vega system lost 6,456 m² (717.36 m² yr⁻¹) in the early twenty-first century (Figs. 6 and
353 7; Table II, supplementary material). One particular case is La Isla Beach, where the
354 progradation process began in the 1990s, increasing by 2,404 m² (171.78 m² yr⁻¹) until
355 2006. In last decade of the twentieth century (1992-2001), the maximum recession took
356 place in Mexota (-3.92 m/-0.44 m yr⁻¹), Sarello (-24.54 m/-2.73 m yr⁻¹), Frejulfe (WP, -
357 0.56 m/-0.06 m yr⁻¹), Carniciega (-1.56 m/-0.09 m yr⁻¹), Espasa (WP, -4.20 m/-0.47 m yr⁻¹),
358 and Vega (CP, -17.28 m/-1.92 m yr⁻¹). However, other dune systems experienced
359 progradation during this time including: Peñarronda (23.27 m/2.59 m yr⁻¹), Frejulfe (EP,
360 10.65 m/1.18 m yr⁻¹), Barayo (12.1 m/1.34 m yr⁻¹), Otur (6.23 m/0.69 m yr⁻¹), La Isla
361 (20.35 m/2.26 m yr⁻¹), Espasa (EP, 3.96 m/0.44 m yr⁻¹), and Vega (EP and WP, 8.58
362 m/0.95 m yr⁻¹) (Fig. 7; Table II, supplementary material).

363 After 2006, a second progradation period occurred in some dune fields with different
364 durations and magnitudes (Figs. 4, 6 and 7). The dunes of Peñarronda, Sarello, Frejulfe,
365 Otur, the western part of Isla, Espasa and Vega all prograded between 2001 to 2006
366 with values ranging from 20.28 m (4.06 m yr⁻¹) to 4.09 m (0.81 m yr⁻¹) (Fig. 7. Table II,
367 supplementary material). Other dune fields featured by recession beginning in 2001 or
368 before, such as Mexota (-2.46 m/-0.49 m yr⁻¹), Barayo (-4.13 m/-0.83 m yr⁻¹), Carniciega
369 (-1.79 m/-0.30 m yr⁻¹) and the eastern part of Isla (-1.51 m/-0.30 m yr⁻¹) (Figs. 4 and 7;
370 Table II, supplementary material).

INSERT FIGURE 7

371

372 However, Barayo and Carniciega began retreating before this period. At 2001 and 2014,
373 the surface decrease was of 10,302.49 m² (792.49 m² yr⁻¹) and 5,151.18 m² (396.24 m²
374 yr⁻¹), respectively (Fig. 7; Table II, supplementary material). Another case is Mexota,
375 because the erosion began in 1992 with a recession of 8241.04 (-374.59 m² yr⁻¹). The
376 same patterns occurred on the eastern side of La Isla, Espasa, and Vega (Figs. 4 and 7;
377 Table II, supplementary material). Since 1992, dune recession has been widespread for
378 these dune fields, repeating this pattern in intervals between 2006 and 2011 and again
379 between 2011 and 2014.

380 Dune fronts have also experienced progressive erosion since the 2009 photograph, with
381 different behaviours shown depending on the dune field studied. The maximum erosion
382 until 2014 is highlighted in Sarello (-17.9 m/-3.58 m yr⁻¹), Frejulfe (-28.04 m/-5.68 m yr⁻¹),
383 Barayo (-18.48 m/-3.69 m yr⁻¹), and Otur (-38.73 m/-7.74 m yr⁻¹). The most important
384 recession occurred in the storms of 2014 and other systems, such as in Peñarronda,
385 Carniciega, and Vega, have all decreased their surface extent (Figs. 4 and 7; Table II,
386 supplementary material). All of these dunes experienced progressive erosion (Fig. 6)
387 which has been attenuated until today

388 **4.3. Specific dune behaviour during the 2013/14 storm period**

389 During the winter of 2013/14, the Cantabrian coast was negatively impacted by frequent
390 high-energy storm wave events, which caused extensive damage to infrastructure and
391 civil works (Flor et al., 2014). These storms produced the erosion of the beach-dune
392 systems, affecting mainly the upper intertidal beaches, the fronts of the dune fields, and
393 surface berms, promoting strong remobilisation of sediment in the nearshore. Authorities
394 have estimated the total cost of cleaning and repairing the damage to be more than 40
395 million euros (Rasilla et al., 2014).

396 In total, four particularly energetic episodes of storm waves occurred. The first was in
397 mid-December 2013 and early January 2014, which did not cause major damage. In
398 early February, another storm caused significant damage due to the combined effect of
399 strong westerly winds, offshore waves of up to 11.3 m and spring high tides of 4.61 m
400 (Table 2). The final and most damaging storm event occurred on the night of March 3rd
401 and 4th. A combination of Atlantic swell waves, local sea wind and spring tides (Rasilla
402 et al., 2014; Flor et al, 2014) lead to a heighten episode of erosion. Strong winds with
403 severe gusts and high offshore waves resulted in a major impact on the coastline; peak
404 gusts exceeded the threshold, which refers to speeds above 120 km h⁻¹ for a period of 3
405 seconds.

406

407

INSERT FIGURE 8

408 The temporal behaviour of the dune dynamics can be explained by the evolutionary
409 models of Hesp (2002). On the one hand, the model best represented is one in which
410 the dune systems had erosion in the dune front (from the centimetric to metre scale),
411 along the entire dune field, or in localised sections (Figs. 8 A and B). Such erosion
412 occurred in Mexota (Fig. 9A), Sarello, Frejulfe, Barayo (Fig. 9C), Otur (Fig. 9D),
413 Quebrantos, Salinas (Fig. 9F), Xagó, Carniciega (Fig. 9G), Rodiles (Fig. 9E), La Isla,
414 Espasa, and Vega (Fig 9H) dune fields. In addition, dune fields where landward migration
415 took place are well differentiated (Fig. 8C), as noted in Peñarronda, Navia (Fig. 9B) and
416 at the eastern end of Xagó with the aeolian advancement of sand bodies. Other small
417 dune fields, such as Angueiro (Fig. 1), have been completely eroded (not included in
418 this study).

419

INSERT FIGURE 9

420

421 The maximum erosion value for dune retreat was measured at Sarello, with an average
422 recession of 40.61 m in WP, where the foredune was largely destroyed. Other systems
423 also significantly damaged included: Otur, undergoing a maximum retreat of 30 m;
424 Barayo, with regression of 18 m and 13.63 m (WP and CP, respectively); and Salinas-El
425 Espartal which showed a maximum in WP and 2.55 and 11.57 m of recession in CP and
426 EP (Fig. 10). In all these cases very steep vertical slopes were generated, in some cases
427 reaching 5 metres in height. In proportion, the incident swell caused steeper slopes in
428 the eastern sectors, which have even had worse recovery later on.

429 Systems where a landward sediment migration was evident by sandy sheets or
430 washover fans, experienced less erosion. For example, Navia, which suffered a
431 recession of between 4.68 m in EP and 1.72 in WP and CP (Table I, supplementary
432 material), Mexota, with 3.40 m, and Xagó, which varied between 6.48 m and 2.91 m in
433 WP and EP, respectively (Fig. 10; Tables I and II, supplementary material).

434 **INSERT FIGURE 10**

435 **5- DISCUSSION**

436 The Asturias coastline is a high-energy, wave-dominated system that, over the last half-
437 century, has experienced a series of particularly strong storm wave events, especially
438 during the years, 1959-60, 1960-61, 1971-72, 1976-77 1977-78, 1982-83, 1983-84,
439 1993-94, 1994-95, and more recently in 2013-2014. (Table 1). In contrast, from 2000 to
440 2005 they have experienced a more quiescent period, promoting an accretionary phase
441 along most of length (Figs. 4, 5 and 7).

442 Estuaries are the main suppliers of sediments for the formation of dunes on the Asturian
443 coast, resulting in the most extensive dune fields located near river mouths. The most
444 obvious case is the Nalon river, which is the most important riverine source of sediment
445 to the Asturian coast (Flor-Blanco and Flor, 2019, García-Ordiales et al, 2020).

446 Prior to anthropogenic impacts during the 20th century (Flor-Blanco et al, 2015a), all
447 anthropized dune fields in Asturias were supplied by large riverine sources. Some such
448 as the Salinas-El Espartal and Xagó systems, grew as a result of a prograding phase
449 since the Flandrian (MIS 1) high stand sea-level, and subsequently by a sea-level fall
450 according to three different stages of evolution (Flor-Blanco et al., 2016). However, those
451 dune fields affected by the construction of jetties recorded considerable progradation in
452 subsequent years (Flor-Blanco et al., 2015a), as opposed to natural shorelines which
453 prograded more slowly.

454 **5.1 Shoreline change**

455 During 20th and 21st centuries, natural dune shorelines in Asturias presented two periods
456 of erosion and progradation. As such, Peñarronda, Mexota, Sarello, Frejulfe, Barayo,
457 Otur, Aguilera, Espasa, and Vega (Fig. 7) showed gradual erosion over several decades
458 (Flor-Blanco et al., 2019).

459 Despite the distinct differences in evolutionary behaviour between natural and human-
460 modified dune fields during the last decades, similar erosional episodes are still apparent
461 (Fig. 11), including a similar morphologic response of the dune front, in terms of triggering
462 vertical erosive slopes or washover lobes. The initial erosive phase occurred between
463 1980 to the 1990s (Flor et al., 2019) followed by a low-energy period of storm waves
464 (2000-2005) and a general progradation of dune systems. Later, since 2006, most dune
465 coasts underwent a more active erosional phase, as shown in Figure 11, where in both
466 anthropic and natural coastlines there were parallel behaviours in terms of change.

467 In the case of the anthropic-influenced dunes, both natural phenomena *and* human
468 management impacts were at play. Consequently, shorelines have been subjected to
469 accelerated erosion. All remaining Cantabrian dune fields have experienced natural
470 retreat in recent decades (Lorenzo et al., 2007; Flor et al., 2011, Flor-Blanco et al., 2015a

471 and b; Flor et al., 2015; Borghero, 2015; de SanJosé et al., 2018) although to a lesser
472 extent in those associated with river mouths and confined by jetties (Fig. 11).

473

INSERT FIGURE 11

474 **5.2 Drivers of shoreline change**

475 Sea level rise measured in Santander (central Cantabrian Sea) for the period of 1943-
476 2010 (García *et al.*, 2012), showed an increase of 2.38 mm yr⁻¹. The estimated present
477 rate of sea-level rise is about 2.08 ± 0.33 mm yr⁻¹ from the tide gauge records at
478 Santander (Chust et al., 2009). Another previous study has highlighted sea-level rise
479 between 2.0 and 4.3 mm y⁻¹ (Lorenzo et al., 2007) as a contributing factor. The
480 occurrence of storms, each time with greater frequency and enhanced intensity, and with
481 increased average wave heights, are also important driving factors in erosion (Conde
482 Criado, 2014; Masselink et al., 2016; Rangel-Buitrago et al., 2016). However, other
483 authors believe that the higher frequency and magnitude of storms in 2013 and 2014
484 have been enhanced by abrupt changes of the Arctic Oscillation (AO), North Atlantic
485 Oscillation (NAO), and East Atlantic Oscillation (EA) phases, changing from a positive to
486 a negative phase without passing through a slower neutral phase (Rangel-Buitrago et
487 al., 2016).

488 In the extreme storms of 2014 and similar to the coastal storm impacts noted on the
489 English (Masselink et al., 2016) and French coasts (Castelle et al., 2015), it is also
490 important to consider the effects of local meteorological tides, which when coincident
491 with storms at their maximum tidal levels may potentially induce an increased erosive
492 impact (Cooper et al., 2004; Guisado-Pintado and Jackson, 2018; 2019). In addition, the
493 impact of extreme storm waves in the Cantabrian Sea during the 2014 winter can be
494 classified as a collision and an overwash regime, as described by Sallenger (2000) for
495 barrier islands.

496 Conde Criado (2014) studied the significant wave heights in the buoy wave station
497 located at NNW of the Peñas Cape (POS05) between the 1st October 2013 and the 10th
498 March 2014, and results showed that 2014's winter storms were exceptional in their
499 recurrence, which is in consonance with our results (Fig. 2). The present study confirms
500 that the key to the erosional power of storm waves in 2013/14 was the higher frequency
501 of $H_s > 3\text{m}$ and in particular, the incidence of events with $H_s > 9\text{ m}$ (Table 1). Flor et al.
502 (2014) have catalogued Asturian coastal damage. Masselink et al. (2016) discussed
503 beach erosion changes in NW Europe, while Castelle et al. (2015) recorded some 22
504 storms with $H_s > H_{s,99\%}$ and 4 storms with $H_s > 9\text{ m}$ during 2013/14, in addition to the fact
505 the Gironde coast was exposed to the most energetic wave conditions over the last 18.3
506 years. In this sense, Castelle et al. (2017) also examined post-storm recovery on those
507 same coasts.

508 **5.3 Dune-fringed shoreline changes**

509 Ultimately, there has been a notable reduction in the area of dune fields remaining along
510 the Cantabrian coast since the 1990s, albeit produced sometimes by anthropic
511 interventions. This pattern of coastal retreat has intensified since 2006, with dune
512 frontage erosion prevalent across most sites presented in this study, mainly due to the
513 recurrence of high-energy storms. The 2014 storms, therefore, represent some of the
514 most destructive periods along the Spanish Atlantic coast in the last two decades and a
515 prominent change in the approach angle (5°) of the storm waves is highlighted as a
516 potential contributing factor that has helped to magnify their erosive impact. To better
517 understand any changes in onshore wave patterns for the whole beach-dune system of
518 the study area, higher resolution bathymetry for each system would have been desirable
519 to allow shallow water numerical wave models to be applied. However, detailed
520 information of the 1996-2014 geomorphologic evolution of the sublittoral region was not
521 available. Nevertheless, in the eastern sector of some dune fields there is evidence of
522 inhibited recovery such as Frexulfe, Barallo or Rodiles, and even the disappearance of

523 the dune morphologies of larger dune fields such as Xagó and Vega. Other studies in
524 open coasts and beaches in estuaries and bays have shown that moderately high waves
525 can cause significantly enhanced erosion due to atypical direction patterns (Mortlock et
526 al., 2017; Harley et al., 2017, Gallop et al., 2020).

527 The future prospects of these dune-fringed coasts in NW Spain are somewhat uncertain.
528 Much of the previously storm-eroded sediment still remains in the nearshore zone of
529 many of the sites studied and therefore post-recovery of the beach-dune systems has
530 not fully taken hold, making future impacts from (even of lower magnitude than previous
531 years) storm activity even more likely. According to Thom and Hall (1991), sediments
532 can gradually return during longer period swells and lower wave events. In recent years
533 (2015-2020) the Cantabrian coast has recorded such lower energy conditions and
534 progradation which may provide a catalyst for recovery in case new higher energy events
535 do not arrive in the near future.

536 Recovery to pre-2014 sediment levels on beaches and dunes are still some way off
537 however, and over the 2015 to 2016 period, only minimal recovery and superficial
538 restoration of beach levels was observed (Flor-Blanco and Flor, 2016). From 2016, there
539 has been a significant reduction in the height of the front dune slopes, and even smaller
540 dune morphologies forming at their base. In the case of the washover lobes, they have
541 seen the proliferation of pioneering dune vegetation (Fig. 12). Therefore, this study
542 represents an advance in our knowledge of the morphodynamics of the dune fields in
543 Asturias so that future more informed-management can be considered (Martínez et al.,
544 2013) or new preventive solutions such as the installation of offshore structures for
545 protection (Abanades et al., 2018).

546 **INSERT FIGURE 12**

547 **6- CONCLUSIONS**

548 The exhaustive wave analyses carried out demonstrates a significant increase in storm
549 wave activity especially during 2014. From 1993 to 1994, high-energy storm events
550 dominated, whilst the 2000-2005 period corresponded to a relatively low energy phase.
551 Subsequently, storm wave events became more frequent. Since 2006, almost all dune
552 fields were decreasing in extent, coinciding with this new, higher-energy and erosional
553 phase.

554 In particular, 2013/14 saw a higher frequency of storm events with offshore $H_s > 3\text{m}$, and
555 more importantly, a high recurrence of storm events with offshore $H_s > 9\text{ m}$. Offshore
556 approach direction of storm waves also switched 5° to the west, thereby modifying the
557 wave propagation pattern and incidence angle over the coastal dune-beach systems. In
558 February and March 2014, waves reached a maximum height of up to 11 m offshore,
559 which was combined with spring high tides and a localised wave orientation change,
560 favouring enhanced erosional events and thus triggering the removal of small dune
561 areas, some of them located in the eastern margin of the most important dune fields.
562 This is evident in those beach/dune systems whose orientation is NE-SW or E-W and
563 which, in addition, have a well-developed rocky outcrop on the western margin.

564 All coastal dune stretches saw enhanced erosion from 2011-2014, including more
565 intensify levels during the winter of 2014, with the greatest impact on Peñarronda,
566 Sarello, Frejulfe, Barayo, Otur, Carniciega, and La Isla dune coasts, reaching up to a
567 maximum horizontal shoreline retreat of 40 m. Eroded sand was relocated into the
568 foreshore and backshore, zones even forming pioneer dunes adjacent to the 2014 dune
569 scarps.

570 This succession of more intense storm wave activity in the last decade is perhaps
571 evidence of climate change impacts on the Cantabrian coast detected in other parts of
572 the world and for this reason, the dune front has been receding since 2006.

573 The future of most of these fragile coastal dune systems, which are protected habitats
574 (Gracia et al., 2009), is uncertain because coastalline recession is now prevalent in all
575 Asturias's dune-fringed coasts. This study highlights how dune coasts can dynamically
576 respond to storm impact from heightened wave conditions as well as a small alteration
577 in normal storm conditions (approach direction), helping tip coastlines into highly
578 erosional phases. Understanding the behaviour of these coastlines therefore is now even
579 more important in future coastal dune management approaches.

580 **Acknowledgments**

581 Wave data bases from Estaca de Bares and Cabo de Peñas buoys, as well as from
582 WAM numerical model, have been supplied by Puertos del Estado (Spanish
583 Government). Aerial photographs and orthophotographs have been supplied by the
584 Cartography Service of the Principado de Asturias and the Instituto Geográfico Nacional
585 (IGN) of Spain. The digital elevation model has been provided by the Cartography
586 Service of the Principado de Asturias (SITMA). The authors also thank the Cluster of
587 Energy, Environment and Climate Change and to the Marine Observatory of the
588 University of Oviedo for providing the Cudillero buoy data. In addition, we would like to
589 thank the invaluable help of Monica Cardo with several graphics and the scientific
590 reviewers have been helpful in improving the manuscript

591 This work is a contribution to UNESCO IGCP Project 639 'Sea Level Change from
592 Minutes to Millennia'.

593 **Bibliography**

594 Abanades, J., Flor-Blanco, G., Flor, G., Iglesias, G. 2018. Dual wave farms for energy
595 production and coastal protection. *Ocean Coast Manage.* 160, 18-29.

596 Alonso, I, Alcántara-Carrió, J, Cabrera, L. 2002. Tourist resorts and their impact on
597 beach erosion at Sotavento beaches, Fuerteventura. Spain. *J Coastal Res.* SI 36, 1-7.

598 An, L., Che, H., Xue, M., Zhang, T., Wang, H., Wang, Y., Zhou, C., Zhao, H., Gui, K.,
599 Zheng, Y., Sun, T., Liang, Y., Sun, E., Zhang, H., and Zhang, X. 2018. Temporal and
600 spatial variations in sand and dust storm events in East Asia from 2007 to 2016:
601 Relationships with surface conditions and climate change. *Sci Total Environ.* 633, 452-
602 462.

603 Anfuso, G., Loureiro, C., Taaouati, M., Smyth, T.A.G., Jackson, D.W.T. 2020. Spatial
604 variability of beach impact from post-tropical cyclone Katia (2011) on Northern Ireland's
605 north coast. *Water.* 12(5), 1380. <https://doi.org/10.3390/w12051380>.

606 Anthony, E. J. 2013. Storms, shoreface morphodynamics, sand supply, and the accretion
607 and erosion of coastal dune barriers in the southern North Sea. *Geomorphology.* 199, 8-
608 21.

609 Aubrey, DA, Ross, RM. 1985. The quantitative description of beach cycles. *Mar Geol.*
610 69, 155-170.

611 Augustinus, P. G. E. F. 2003. Coastal systems. Theme, 6. Vol I.

612 Borghero, C. 2015. Study of morphological evolution of dune fields in Cantabria (N.
613 Spain) during the Anthropocene. Master Thesis, University of Uppsala. [http://www.diva-](http://www.diva-portal.org/smash/get/diva2:848962/FULLTEXT01.pdf)
614 [portal.org/smash/get/diva2:848962/FULLTEXT01.pdf](http://www.diva-portal.org/smash/get/diva2:848962/FULLTEXT01.pdf)

615 Carretero, JC, Gomez, M., Lozano, I, De Elvira, AR. 1998. Changing waves and storms
616 in the Northeast Atlantic?. *Bulletin of the American Meteorological Society.* 79(5): 741-
617 760.

618 Carter, RWG. 1991. Near-future sea level impacts on coastal dune landscapes.
619 *Landscape Ecol.* 6 (1/2): 29-39.

620 Carter, RWG, Hesp, PA, Nordstrom, KF. 1990. Erosional landforms in coastal dunes. In:
621 K.F. Nordstrom, N.P. Psuty and B. Carter (Eds). *Coastal Dunes, Form and Process:*
622 *Wiley*, pp. 217-250.

623 Chaaban, F., Darwishe, H., Battiau-Queney, Y., Louche, B., Masson, E., El Khattabi, J.,
624 Carlier, E. 2012. Using ArcGIS® modelbuilder and aerial photographs to measure
625 coastline retreat and advance: North of France. *J Coastal Res.* 28(6), 1567-1579.

626 Castelle, B., Marieu, V., Bujan, S., Splinter, K. D., Robinet, A., Sénéchal, N., Ferreira, S.
627 2015. Impact of the winter 2013–2014 series of severe Western Europe storms on a
628 double-barred sandy coast: Beach and dune erosion and megacusp embayments.
629 *Geomorphology.* 238, 135-148.

630 Castelle, B., Bujan, S., Ferreira, S., Dodet, G. 2017. Foredune morphological changes
631 and beach recovery from the extreme 2013/2014 winter at a high-energy sandy coast.
632 *Mar Geol.* 385, 41-55.

633 Castelle, B. and Harley, M. 2020. Extreme events: impact and recovery. In: Jackson,
634 DWT and Short, AD (Eds) *Sandy Beach Morphodynamics*, Elsevier, Amsterdam.

635 Church, JA, Clark, PU, Cazenave, A, Gregory, JM, Jevrejeva, S, Levermann, A,
636 Merrifield, MA, Milne, GA, Nerem, RS, Nunn, PD, Payne, AJ, Pfeffer, WT, Stammer, D,
637 Unnikrishnan, AS. 2013. Sea-level rise by 2100. *Science*, 342 (6165), pp. 1445-1445.

638 Chust, G., Borja, Á., Liria, P., Galparsoro, I., Marcos, M., Caballero, A., Castro, R. 2009.
639 Human impacts overwhelm the effects of sea-level rise on Basque coastal habitats (N
640 Spain) between 1954 and 2004. *Estuar Coast Shelf S.* 84, 453-462.

641 Ciavola, P., Ferreira, O., Haerens, P., Van Koningsveld, M., Armaroli, C. 2011. Storm
642 impacts along European coastlines. Part 2: lessons learned from the MICORE project.
643 *Environ Sci Policy.* 14(7), 924-933.

644 Cid, A, Menéndez, M, Castanedo, S, Abascal, AJ, Méndez, FJ, Medina, R. 2016. Long-
645 term changes in the frequency, intensity and duration of extreme storm surge events in
646 southern Europe. *Clim Dynam.* 46(5-6), 1503-1516.

647 Conde Criado, J. 2014. Episodios de oleaje intenso en las costas del Cantábrico durante
648 el periodo octubre-1957 a marzo 2014. AEMET.

649 Cooper JAG, Jackson DWT, Navas F, McKenna J, Malvarez G. 2004 Identifying storm
650 impacts on an embayed, high-energy coastline: examples from western Ireland. *Mar*
651 *Geol.* 210, 261–280.

652 Crapoulet, A, Héquette, A, Levoy, F, Bretel, P. 2015. Évaluation de l'évolution du trait de
653 côte et du bilan sédimentaire littoral en baie de Wissant (Nord de la France) par LiDAR
654 aéroporté. *Geomorphologie.* 21(4), 313-330.

655 Dail, HJ, Merrifield, MA, Bevis, M. 2000. Steep beach morphology changes due to
656 energetic wave forcing. *Mar Geol.* 162, 443-458.

657 Davis, RA, Fox, W.T. 1972. Coastal processes and nearshore sand bars. *Journal of*
658 *Sedimentary Petrology.* 42, 402-412.

659 de Sanjosé Blasco, J., Gómez-Lende, M., Sánchez-Fernández, M., & Serrano-Cañadas,
660 E. 2018. Monitoring Retreat of Coastal Sandy Systems Using Geomatics Techniques:
661 Somo Beach (Cantabrian Coast, Spain, 1875–2017). *Remote Sens-Basel.* 10(9), 1500.

662 Domínguez-Cuesta, M. J., Jiménez-Sánchez, M., González-Fernández, J. A., Quintana,
663 L., Flor, G., Flor-Blanco, G. 2015. GIS as a tool to detect flat erosional surfaces in coastal
664 areas: a case study in North Spain. *Geol Acta.* 13(2), 97-106.

665 Fenster, MS, Dolan, R, Morton, RA. 2001. Coastal storms and shoreline change: signal
666 or noise?. *J Coastal Res.* 17(3), 714-720.

667 Flor, G. 1978. Relación entre la distribución de sedimentos y la circulación costera en la
668 región del Cabo Peñas. *Trabajos de Geología.* (10), 183-195.

669 Flor, G.; Llera, E. M^a; Ortea, J. A. 1982. Los carbonatos biogénicos de los sedimentos
670 de las playas arenosas de Asturias y Cantabria: su origen y significado dinámico.
671 *Cuadernos del CRINAS,* 2.

672 Flor, G, Martínez Cedrún, P, Flor-Blanco, G. 2011. Campos dunares de Asturias,
673 Cantabria y País Vasco, in: Sanjaume, E., Gracia, FJ, (Eds.), Las dunas en España.
674 Sociedad Española de Geomorfología, pp. 127-159.

675 Flor, G, Flor-Blanco, G. 2014a. Raised beaches in the Cantabrian coast, In: Gutiérrez,
676 F., Gutiérrez, M. (Eds.), Landscapes and landforms of Spain. Springer Netherlands; pp.
677 239-248.

678 Flor, G, Flor-Blanco, G. 2014b. Componentes de viento generadores de morfologías y
679 campos de dunas costeras en Asturias (NO de España). Cuaternario y Geomorfología
680 28(3-4); 47-68.

681 Flor, G, Flor-Blanco, G, Flores-Soriano, C. 2014. Cambios ambientales por los
682 temporales de invierno de 2014 en la costa asturiana (NO de España). Trabajos de
683 Geología. 34, 97-123.

684 Flor, G, Flor-Blanco, G, Rey, J. 2015. Dynamics and morpho-sedimentary interactions in
685 the lower mesotidal estuary of Villaviciosa (NW Spain): A management dredging model.
686 Geol Acta. 13(2), 107-121.

687 Flor, G., Flor-Blanco, G., Cedrún, P. M., Flores-Soriano, C., Borghero, C. 2019. Aeolian
688 Dune Fields in the Coasts of Asturias and Cantabria (Spain, NW Iberian Peninsula), in:
689 Morales, J. A. (Ed.). The Spanish Coastal Systems Springer, Cham, pp. 585-609.

690 Flor-Blanco, G, Flor, G. 2016. Management of dune fields on the coasts of Asturias,
691 Cantabria and the Basque Country (Cantabrian Sea, NW Iberian Peninsula), in: Roig
692 Munar (Ed), Restoration and management of dune systems. Case studies; 35-70.

693 Flor-Blanco, G, Flor, G, Pando, L. 2013. Evolution of the Salinas-El Espartal and Xagó
694 beach/dune systems in North-Western Spain over recent decades: evidence for
695 responses to natural processes and anthropogenic interventions. Geo-Mar Lett. 33(2-3),
696 143-157.

697 Flor-Blanco, G, Pando, L, Flor, G, Morales, JA. 2015a. Evolution of beach-dune fields
698 systems following the construction of jetties in estuarine mouths (Cantabrian coast, NW
699 Spain). *Environ Earth Sci.* 73, 1317-1330.

700 Flor-Blanco, G, Flor, G, Pando, L, Abanades, J. 2015b. Morphodynamics, sedimentary
701 and anthropogenic influences in the San Vicente de la Barquera estuary (North coast of
702 Spain). *Geologica Acta* 13 (4): 279-296.

703 Flor-Blanco, G, Rubio-Melendi, D, Flor, G, Fernández-Álvarez, JP, Jackson, DWT. 2016.
704 Holocene evolution of the Xagó dune field (Asturias, NW Spain) reconstructed by means
705 of morphological mapping and ground penetrating radar surveys. *Geo-Mar. Lett.* 36, 35-
706 50.

707 Flor-Blanco, G., Flor, G. 2019. Cantabrian estuaries, in: Morales, J. A. (Ed.), *The Spanish
708 Coastal Systems* Springer, Cham, Springer, Cham, pp. 415-436.

709 Fontán-Bouzas, A, Alcántara-Carrió, J, Correa, ID. 2009. Combined beach-inner shelf
710 erosion in short and medium term (Maspalomas, Canary Islands). *Geol Acta.* 4, 411-426.

711 Fontán-Bouzas, A, Alcántara-Carrió, J. Montoya Montes, J, Barranco Ojeda, A.
712 Albarracín, S, Rey Díaz de Rada, J, Rey Salgado, J. 2013. Distribution and thickness of
713 sedimentary facies in the coastal dune, beach and nearshore sedimentary system of
714 Maspalomas, Canary Islands. *Geo-Mar Lett.* 33, 117-127.

715 Fontán-Bouzas, A., Alcántara-Carrió, J., Albarracín, S., Baptisa, P., Silva, P.A., Portz,
716 L., Portantiolo, R.M. 2019. Multiannual shore morphodynamics of a cusped foreland:
717 Maspalomas (Gran Canaria, Canary Islands). *J Mar Sci Eng.* 7 (11), 416.

718 Gallop, S. L., Vila-Concejo, A., Fellowes, T. E., Harley, M. D., Rahbani, M., & Largier, J.
719 L. 2020. Wave direction shift triggered severe erosion of beaches in estuaries and bays
720 with limited post-storm recovery. *Earth Surf Proc Land.* 45(15), 3854-3868. DOI:
721 10.1002/esp.5005.

722 García, MJ, Tel, E, Molinero, J. 2012. Sea-level variations on the north and northwest
723 coasts of Spain. *ICES J. Mar. Science*. 69(5), 720-727.

724 García-Ordiales, E., Flor-Blanco, G., Roqueñí, N., Covelli, S., Cienfuegos, P., Álvarez,
725 R. Loredó, J. 2020. Anthropocene footprint in the Nalón estuarine sediments (northern
726 Spain). *Marine Geology*, 106167.

727 Goldenberg, SB, Landsea, CW, Mestas-Nuñez, AM, Gray, WM. 2001. The recent
728 increase in Atlantic hurricane activity: Causes and implications. *Science*. 293(5529),
729 474-479.

730 Gracia, FJ, Sanjaume, E, Calvento, LH, Cordero, AIH, Flor, G, Gómez-Serrano, MÁ, del
731 Río, L. 2009. Dunas marítimas y continentales. In: *Bases ecológicas preliminares para*
732 *la conservación de los tipos de hábitat de interés comunitario en España*. Ministerio de
733 *Medio Ambiente y Medio Rural y Marino de España*, pp. 1-106.

734 Guisado-Pintado, E. and Jackson, DWT. 2018. Multi-scale variability of Storm Ophelia
735 2017: the importance of synchronised environmental variables in coastal impact. *Sci*
736 *Total Environ*. 630, 287-301.

737 Guisado-Pintado, E., Jackson, DWT. 2019. Coastal impact from high-energy events and
738 the importance of concurrent forcing parameters: The cases of Storm Ophelia (2017)
739 and Storm Hector (2018) in NW Ireland. *Front Earth Sc-Switz*. 7, 190. doi:
740 10.3389/feart.2019.00190.

755 Harley M.D, Turner, I.L, Kinsela, M.A, Middleton, J.H, Mumford, P.J, Splinter, K.D,
756 Phillips, M.S, Simmons, J.A, Hanslow, D.J, Short, A.D. 2017. Extreme coastal erosion
757 enhanced by anomalous extratropical stormwave direction. *Sci Rep-UK*. 7,1–9.

758 Hernández-Cordero, A. I., Hernández-Calvento, L., Hesp, P. A., Pérez-Chacón, E. 2018.
759 Geomorphological changes in an arid transgressive coastal dune field due to natural
760 processes and human impacts. *Earth Surf Proc Land*. 43(10), 2167-2180.

761 Hesp, P. 2002. Foredunes and blowouts: initiation, geomorphology, and dynamics.
762 *Geomorphology*. 48, 245-268.

763 Hesp, P.A. 2011. Dune coasts, in: E. Wolansky, E., McLusky, D.S. (Eds.), *Treatise on*
764 *Estuarine and Coastal Science* 3. Waltham: Academic Press, pp. 193-221. DOI:
765 10.1016/B978-0-12-374711-2.00310-7

766 Hesp, P.A, Smyth, T.A. 2016. Surfzone-Beach-Dune interactions: Flow and Sediment
767 Transport across the Intertidal Beach and Backshore. *J Coastal Res.* 75, 8-12.

768 Hill, H.W., Kelley, J.T., Belknap, D.F., Dickson, S.M. 2004: The effects of storms and
769 storm-generated currents on sand beaches in Southern Maine, USA. *Mar Geol.* 210,
770 149-168.

771 IPCC Climate Change, 2014. Synthesis report. Contribution of Working Groups I, II and
772 III to the Fifth Assessment Report of the Intergovernmental Panel on Climate Change.
773 2014.

774 Lorenzo, F., Alonso, A, Pagés, J.L. 2007. Erosion and accretion of beach and spit
775 systems in Northwest Spain: a response to human activity. *J Coastal Res.* 23(4), 834-
776 845.

777 Jackson, D.W.T., Short, A.D (Eds.) 2020. *Sandy Beach Morphodynamics*. Elsevier,
778 Amsterdam.

779 Komar, P.D., Allan, J.C. 2008. Increasing hurricane-generated wave heights along the
780 US east coast and their climate controls. *J Coastal Res.* 24(2), 479-488.

781 Lee, G., Nicholls, R., Birkemeier, W.A. 1998. Storm-driven variability of the beach-
782 nearshore profile at Duck North Carolina, USA, 1981–1991. *Mar Geol.* 148, 163-177.

783 López-Fernández, C., Llana-Fúnez, S., Fernández-Viejo, G., Domínguez-Cuesta, M. J.,
784 Díaz-Díaz, L.M. 2020. Comprehensive characterization of elevated coastal platforms in

785 the north Iberian margin: A new template to quantify uplift rates and tectonic patterns.
786 Geomorphology. 364, 107242.

787 Loureiro, C, Ferreira, O, Cooper, J.A.G. 2014. Non-uniformity of storm impacts on three
788 high-energy embayed beaches. *J Coastal Res.* 70(SP1), 326-331.

789 Martínez, M.L., Gallego-Fernández, J.B., Hesp, PA. 2013. Restoration of Coastal Dunes.
790 Springer Science & Business Media.

791 Masselink, G., Scott, T., Poate, T., Russell, P., Davidson, M., Conley, D. 2016. The
792 extreme 2013/2014 winter storms: hydrodynamic forcing and coastal response along the
793 southwest coast of England. *Earth Surf Proc Land.* 41(3), 378-391.

794 Mortlock, T.R., Goodwin, I.D., McAneney, J.K., Roche, K. 2017. The June 2016
795 Australian East Coast Low: Importance of wave direction for coastal erosion assessment.
796 *Water-Sui.* 9(2), 121.

797 Nordstrom, K.F. 1980. Cyclic and seasonal beach response: a comparison of ocean side
798 and bayside beaches. *Phys Geogr.* 1, 177-196.

799 Plomaritis, T.A, Benavente, J, Laiz, I, Del Río, L. 2015. Variability in storm climate along
800 the Gulf of Cadiz: the role of large scale atmospheric forcing and implications to coastal
801 hazards. *Clim Dynam.* 45(9-10), 2499-2514.

802 Rangel-Buitrago, N., Anfuso, G. 2013. Winter wave climate, storms and regional cycles:
803 the SW Spanish Atlantic coast. *Int J Climatol.* 33(9), 2142-2156.

804 Rangel-Buitrago, N.G, Thomas, T, Phillips, M.R, Anfuso, G, Williams, A.T. 2016. Wave
805 Climate, Storminess, and Northern Hemisphere Teleconnection Patterns Influences: The
806 Outer Bristol Channel, South Wales, UK. *J Coastal Res.* 32(6), 1262–1276.

807 Rasilla, D.F., Garmendia, C., García Codrón, J.C., Rivas, V. 2014. Marine storms and
808 coastal risk along the Gulf of Biscay area: winter 2014. *Multidimensao e territórios de*
809 *Risco, Guimaraes (Portugal), Imprensa da Universidade de Coimbra,* 336-342.

810 Rasilla, D., García-Codron, J.C., Garmendia, C., Herrera, S., Rivas, V. (2018). Extreme
811 Wave Storms and Atmospheric Variability at the Spanish Coast of the Bay of Biscay.
812 Atmosphere-Basel. 9(8), 316.

813 Rodríguez-Ramírez, A., Morales, J.A., Delgado, I., Cantano, M. 2008. The impact of man
814 on the morphodynamics of the Huelva coast (SW Spain). J Iber Geol. 34(2), 313-327.

815 Ruggiero P., Kaminsky M.G., Gelfenbaum G., Voigt B. 2005. Seasonal to interannual
816 morphodynamics along a high-energy dissipative littoral cell. J Coastal Res. 21(3), 553-
817 578.

818 Ruz, M.H., Anthony, E.J., Faucon, L. 2005. Coastal dune evolution on a shoreline subject
819 to strong human pressure: the Dunkirk area, northern France, in: Proceedings Dunes
820 and Estuaries Int. Conf. Natu. Restaur. Pract. in European Coast. Habit. Koksijde,
821 Belgium, pp. 441-449

822 Sallenger Jr, A.H. 2000. Storm impact scale for barrier islands. J Coastal Res. 16(3),
823 890-895.

824 Sanjaume, E, Gracia, F.J (Eds.). 2011. Las dunas de España. Sociedad Española de
825 Geomorfología, Madrid.

826 Senechal, N., Ruiz de Alegría-Arzaburu, A. 2020. Seasonal imprint on beach
827 morphodynamics, In: Jackson, D.W.T., Short, A.D (Eds.) Sandy Beach
828 Morphodynamics, Elsevier, Amsterdam.

829 Short, AD. Hesp, PA. 1982. Wave, beach and dune interactions in southern Australia.
830 Mar Geol. 48, 259-284.

831 Short, A.D., Jackson, D.W.T. 2021. Beach Morphodynamics. In: Reference Module in
832 Earth Systems and Environmental Sciences. Elsevier. Amsterdam.
833 <https://doi.org/10.1016/B978-0-12-818234-5.00052-3>

839 Thom B.G., Hall W. 1991. Behaviour of beach profiles during accretion and erosion
840 dominated periods. *Earth Surf Proc Land*. 16, 113–127.

841 Trindade, J., Ramos-Pereira, A. 2013. Inundation and erosion susceptibility in wave
842 dominated beaches. *Finisterra*. 95, 83-104.

843 Vousdoukas, M.I., Voukouvalas, E., Annunziato, A., Giardino, A., Feyen, L.A. 2015.
844 European storm surge model for projections of extreme water levels under climate
845 change scenarios. European Commission.

846 Vousdoukas, M.I., Mentaschi, L., Voukouvalas, E., Verlaan, M., Feyen, L. 2017. Extreme
847 sea levels on the rise along Europe's coasts. *Earths Future*. 5(3), 304-323.

848 Von Storch, H., Woth, K. 2008. Storm surges: perspectives and options. *Sustainability*.
849 *Science*. 3(1), 33-43.

850 Wright, L.D., Short, A. 1984. Morphodynamic variability of surf zones and beaches: A
851 synthesis. *Mar Geol*. 56, 93-118.

852 Yates, M.L., Guza, R.T., O'Reilly, W.C., Seymour, R.J. 2009a. Overview of seasonal sand
853 level changes on southern California beaches. *Shore and Beach*. 77(1), 39-46.

854 Yates, M.L., Guza, R.T., O'Reilly, W.C. 2009b. Equilibrium shoreline response:
855 Observations and modeling. *J Geophys Res*. 114, C09014. doi: 10.1029/2009JC005359.

856 Zoulas, J.G. 2008. Beach changes in the San Pedro littoral cell, Southern California.
857 UMO Microform 3343338. ProQuest LL.C. Univ. of California, Los Angeles, 1930-2007.

858

859 TABLES.

860 Table 1. Percentage distribution of storm wave events obtained from the WAM numerical
861 model for the whole period (1st July 1958 - 30th June 2015), and for the nine climatic
862 years with highest total annual energy.

863 Table 2. Maximum significant height recorded (m) in Cape Peñas buoy and tidal ranges
864 (m) recorded in Musel Port (Source: Puertos del estado. Ministerio de Fomento).

865 FIGURES

866 Figure 1. Location of the studied Asturian dune fields (black circles) and the riverine
867 fluvial sources of sediments. 1) Peñarronda, 2) Mexota, 3) Sarello, 4) Navia, 5) Frejulfe,
868 6) Barayo, 7) Otur, 8) Quebrantos, 9) Salinas-El Espartal, 10) Xagó, 11) Carniciega, 12)
869 Rodiles, 13) La Isla, 14) Espasa, 15) Vega. Dune field removed (grey circle): Angueiro.

870 Figure 2. Statistics of storm events ($H_s > 3\text{m}$) for each climatic year from 1958-1959 to
871 2014-2015: A) Maximum H_s ; B) Maximum energy of a storm event; C) Number of storm
872 events; D) Total duration for the whole of storm events; E) Maximum duration of a storm
873 event; F) Average duration of storm events; and G) Total annual energy. Data for each
874 climatic year is plotted as corresponding to its starting year (i.e. data for climatic year
875 2014-2015 are plotted as corresponding to 2014). H_s is in m, duration in hours (h) and
876 energy in $\times 10^6 \text{ J/m}^2$. The dashed line indicates the climatic year 2013-2014.

877 Figure 3. Directional histograms of storm waves ($H_s > 3\text{m}$) for A) the 1958-2015 period,
878 and B) the climatic year 2013-2014. Directional histograms of extreme storm waves
879 ($H_s > 7\text{m}$) for C) the 1958-2015 period, and D) the climatic year 2013-2014.

880 Figure 4. Evolution (1992-2014) of the beach-dune shoreline and location of measured
881 profiles for each dune field. Orthophotographs are 2011. Dune coastlines include: a)
882 Peñarronda, b) Mexota, c) Sarello, d) Navia, e) Frejulfe, f) Barayo, g) Otur, h)

883 Quebrantos, i) Salinas-El Espartal, j) Xagó, k) Carniciega, l) Rodiles, m) La Isla, n)
884 Espasa and o) Vega.

885 Figure 5. Shoreline evolution and surface area changes at human-impacted dune sites.
886 The dashed red line represents changes in dune field area from 1992 until 2014.
887 Accretion/erosion rates (m yr^{-1}) are shown for the three profiles established at each
888 dune/beach system.

889 Figure 6. Surface variations (m^2) of dune fields studied, comparing three representative
890 moments: 1992 (blue), 2006 (red) and 2014 (green).

891 Figure 7. Shoreline evolution and surface area changes at natural sites. The dashed red
892 line represents changes in dune field area from 1992 until 2014. Accretion/erosion rates
893 (m yr^{-1}) are shown for the three profiles established at each dune/beach system.

894 Figure 8. Conceptual models of beach dunes response to 2013-2014 storm waves
895 (without scale). Based in Hesp (2002).

896 Figure 9. Photographs were taken on April of 2014 (west to east): A) Mexota. Climbing
897 dune eroded since 70s, nowadays with a high slope, B) Navia, foredune confined by
898 jetties. In 2014 some fan lobe covered the dune field, C) Barayo foredune lost until 18 m
899 in 2014 surge storms, D) Otur was the dune field more affected by 2014 wave storms (-
900 35 m), E) East of Rodiles foredune, with recession of 14.54 m in 2014, F) El Espartal
901 retreated until 13 m since 2014, influenced by port management G) Carniciega climbing
902 dune with a recession of 12.60 m in 2014, H) Vega foredune was one of the most
903 damaged (-7 m). On the beach, a fallen milestone (demarcation line) of the terrestrial
904 public domain (Spanish Coastal Law).

905 Figure 10. Surface variations (m^2) of dune fields studied after the greatest wave storms
906 during winter of 2014, comparing two periods: 2011 (purple), and 2014 (green).

907 Figure 11. Statistics of surface averaged evolution during 1990's to 2014. A) Natural
908 dunes, B) Anthropic-influenced dunes.

909 **Figure 12.** Photographs were taken during 2020 (west to east) showing shoreline
910 recovery of sites shown previously in figure 9: A) Mexota. Increased sedimentary volume
911 on the beach and attenuated recession, B) Navia, after continuous overflows in recent
912 years, the dune migrates landward (photograph provided by Efrén García Ordiales), C)
913 Barayo. Dune intervened as part of the Life + Arcos project. re-profiling activities, D)
914 Otur. Slope reduction (3 m high in 2014) and generation of a new foredune with pioneer
915 vegetation at its base, E) East of Rodiles. Great sedimentary increase on the beach and
916 generation of vegetated dunes at its base, F) El Espartal. Sedimentary increase on the
917 beach, less accelerated recession and dependent on dredging from Avilés estuary, G)
918 Carniciega. Continued recession but with more sediment on the beach, slope decreased,
919 H) Vega. Foredune recession ceased (Life + Arcos project) and dunes developing
920 pioneer vegetation.

921

922

923

924

925

926

927

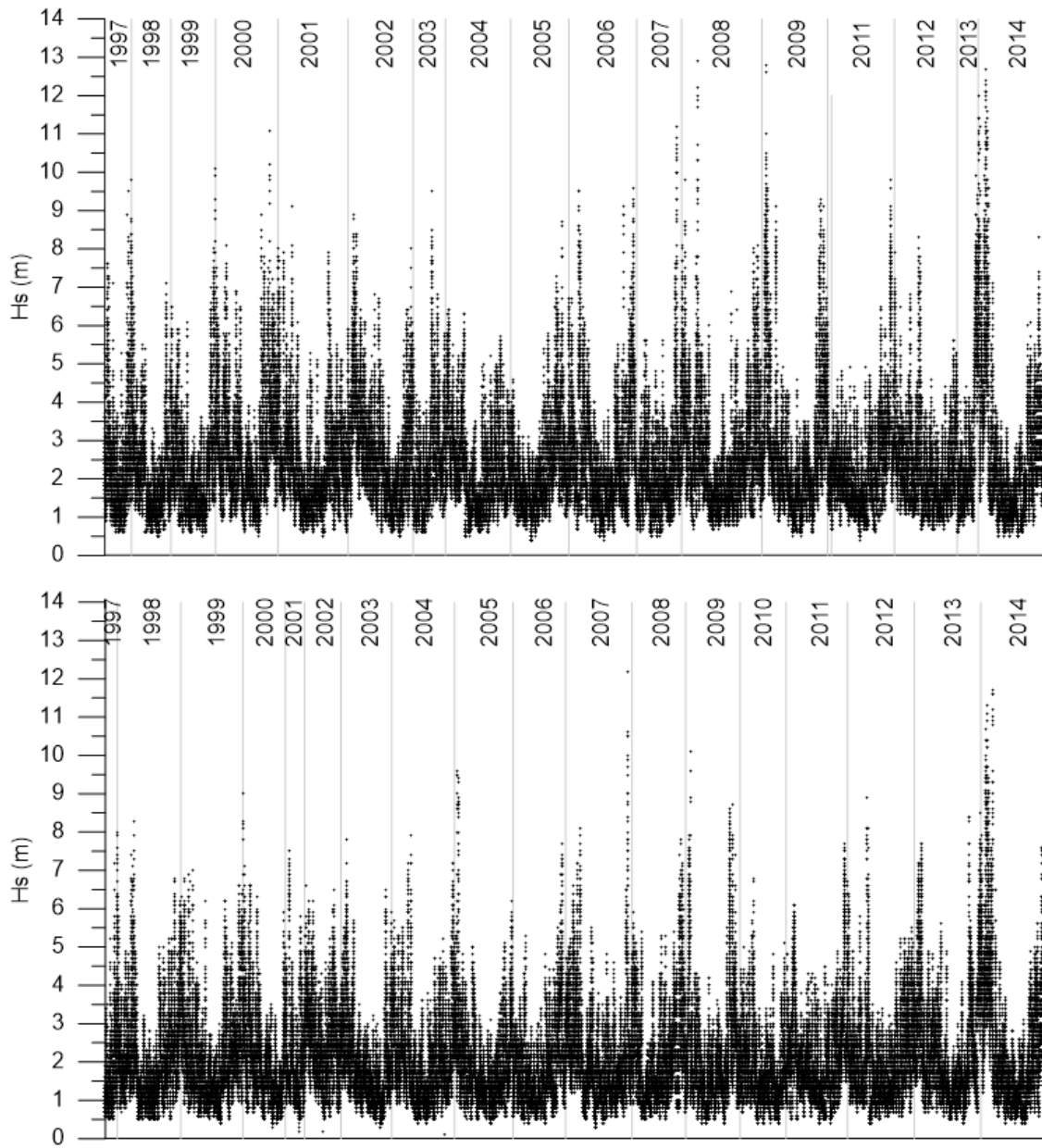
928

929

930

931

932



934

935 Figure I, supplementary material. Wave distribution (1997-2014) obtained from Estaca de Bares
936 (top) and Cabo de Peñas (bottom) buoys

937

	DUNE FIELD	Navia	Quebrantos	Salinas-El Espartal	Xagó	Rodiles
Years	Measurement dates: Surface (m ²) - Surface difference between recorded years (m ²)					
1992	Surface	73291.94	268430.42	643003.00	425519.7	155800.54
2001	Surface	67987.63	245927.76	421053.81	432659.24	164543.5
	Difference 1992-2001	-5304.31	-22502.66	-221949.19	7139.54	8742.96
2006	Surface	71424.27	244596.00	498395.60	455119.97	172230.76
	Difference 2001-2006	3436.64	-1331.76	77341.79	22460.73	7687.26
2009	Surface	71620.86	242854.03	497071.62	448348.70	173109.17
	Difference 2006-2009	196.59	-1741.97	-1323.98	-6771.27	878.41
2011	Surface	74687.88	242927.7	495886.57	453069.35	178688.61
	Difference 2009-2011	3067.02	73.67	-1185.05	4720.65	5579.44
2014	Surface	73493.97	234436.52	483375.02	417374.16	176001.17
	Difference 2009-2011	-1193.91	-8491.18	-12511.55	-35695.19	-2687.44

	DUNE FIELD	Navia	Quebrantos	Salinas-El Espartal	Xagó	Rodiles
Years	Measurement dates: Accretion/recession rates (m/yr) for each profile					
1992	INITIAL MEASUREMENT					
2001	WP	-3.56/-0.51	6.99/1.00	-11.36/-1.26	0.95/0.11	6.45/0.72
	CP	5.03/0.72	10.64/1.52	-9.89/-1.10	8.39/0.93	11.36/1.26
	EP	-8.26/-1.18	13.36/1.91	-3.90/-0.43	1.4/0.16	14.16/1.57
2006	WP	3.52/0.70	5.71/1.14	-4.50/-0.90	26.26/5.25	14.88/2.98
	CP	6.39/1.28	5.73/1.15	-4.23/-0.85	9.52/1.90	15.66/3.13
	EP	7.86/1.57	8.39/1.68	-2.00/-0.40	4.86/0.97	5.20/1.04
2009	WP	-0.95/-0.32	0.00	-1.81/-0.60	-12.48/-4.16	0.10/0.03
	CP	1.41/0.47	-0.88/-0.29	-2.02/-0.67	-4.70/-1.57	2.38/0.79
	EP	-0.10/-0.03	-2.71/-0.90	0.00/0.00	0.39/0.13	-0.08/-0.03
2011	WP	-0.5/-0.25	0.38/0.19	-2.33/-1.17	-1.26/-0.63	1.96/0.98
	CP	-4.09/-2.05	-3.00/-1.50	-2.42/-1.21	3.45/1.72	3.41/1.71
	EP	2.98/1.49	-1.21/-0.60	-0.30/-0.15	2.74/1.37	0.10/0.05
2014	WP	-4.68/-1.56	-16.00/-5.33	-12.20/-4.07	-6.48/-2.16	-0.93/-0.31
	CP	-1.72/-0.57	-10.42/-3.47	-13.01/-4.34	-3.13/-1.04	-0.78/-0.26
	EP	-1.77/-0.59	-11.52/-3.84	-4.03/-1.34	-2.91/-0.97	-14.54/-4.85

938

939 Table I Supplementary material. Changes in area (m²) and accretion/erosion rates (m yr⁻¹) for the
940 western (W), central (C) and eastern (E) profile for each anthropized dune field from 1992 to 2014.

941

	Dune field	Peñarronda	Mexota	Sarelo	Frejulfe	Barayo	Otur	Carniciega	La Isla	Espasa	Vega
Year	Measurement dates: Surface (m ²) - Surface difference between recorded years (m ²)										
1992	Surface	70299.01	11663.7	13422.75	49446.96	58952.20	26690.08	12828.15	3836.90	18022.29	76234.60
2001	Surface	76884.80	4190.07	11229.48	54717.43	64340.76	28526.10	12603.98	5532.22	19841.18	69778.40
	Difference 1992-2001	6585.79	-7473.63	-2193.27	5270.47	5388.56	1836.02	-224.17	1695.32	1818.89	-6456.20
2006	Surface	81093.09	4028.72	13191.99	59561.32	63833.34	31337.32	12208.01	6241.75	19601.80	80169.64
	Difference 2001-2006	4208.29	-161.35	1962.51	4843.89	-507.42	2811.22	-395.97	709.53	-239.38	10391.24
2009	Surface	79083.16	3910.97	10363.02	58509.3	62801.24	30499.28	10719.28	5356.82	7311.52	75055.86
	Difference 2006-2009	-2009.93	-117.75	-2828.97	525528.98	-1032.1	-838.04	-1488.73	-884.93	-12290.28	-5113.78
2011	Surface	79288.38	3870.06	9681.86	52289.79	61348.19	29142.25	10039.34	4830.02	15732.67	72964.79
	Difference 2009-2011	205.22	-40.91	-681.16	-532800.51	-1453.05	-1357.03	-679.94	-526.80	8421.15	-2091.07
2014	Surface	76702.38	3422.66	4061.62	48938.04	54038.27	20535.68	8452.80	3723.88	14016.00	68617.11
	Difference 2009-2011	-2586.00	-447.40	-5620.24	-3351.75	-7309.92	-8606.57	-1586.54	-1106.14	-1716.67	-4347.68

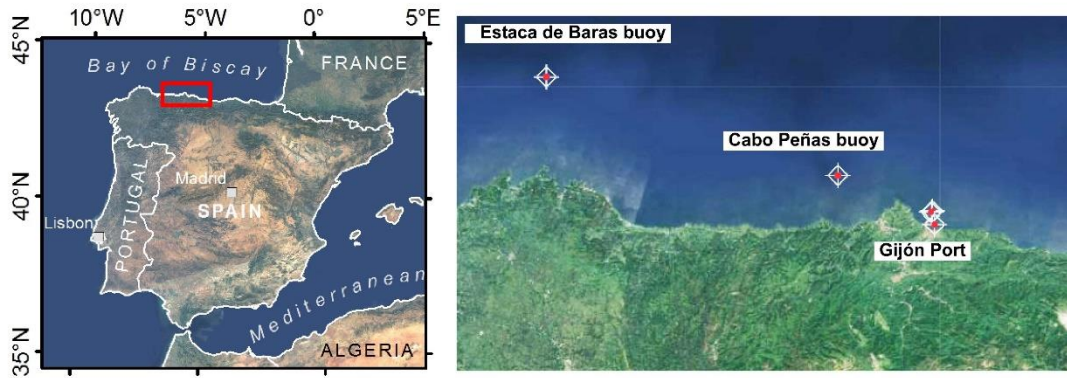
942

	Dune field	Peñarronda	Mexota	Sarelo	Frejulfe	Barayo	Otur	Carniciega	La Isla	Espasa	Vega
Year	Measurement dates: area (m ²) and accretion/recession rates (m/yr) for each profile										
1992	INITIAL MEASUREMENT										
2001	WP	13.00/1.44		-18.06/-2.01	10.83/1.20	1.53/0.17	2.49/0.28	-3.66/-0.41	20.35/2.26	-4.20/-0.47	8.58/0.95
	CP	23.27/2.59	-3.92/-0.44	8.16/0.91	8.16/0.91	3.68/0.41	6.18/0.69	0.00	17.07/1.90	3.96/0.44	-17.28/-1.92
	EP	22.52/2.50		-24.54/-2.73	9.34/1.04	12.1/1.34	7.57/0.84				8.47/0.94
2006	WP	2.12/0.42		21.40/4.28	16.90/3.38	-2.15/-0.43	7.80/1.56	-1.3/-0.26	3.64/0.73	-1.80/-0.36	5.83/1.17
	CP	5.00/1.00	-2.46/-0.49	7.00/1.40	7.00/1.40	-3.52/-0.70	8.30/1.66				13.24/2.65
	EP	19.10/3.82		15.69/3.14	5.50/1.10	-4.13/-0.83	10.89/2.18	-2.03/-0.41	-2.66/-0.53	0.55/0.11	11.96/2.39
2009	WP	0.50/0.17		-13.00/-4.33	-12.05/-4.02	-1.04/-0.35	0.77/0.26	-6.85/-2.28	-1.60/-0.53	-7.06/-2.35	-9.68/-3.06
	CP	2.63/0.88	-1.7/-0.58	-1.43/-0.48	-1.43/-0.48	0.00	0.83/0.28				-10.83/-3.42
	EP	-5.63/-1.88		-11.9/-3.97	11.57/3.86	-1.37/-0.46	-3.88/-1.29	-9.2/-3.07	-4.58/-1.53	-5.10/-1.70	-12.58/-4.19
2011	WP	-1.68/-0.84		-2.85/-1.43	-5.09/-2.55	-0.49/-0.25	-5.75/-2.88	-2.21/-1.11	-2.14/-1.07	-3.65/-1.83	-1.69/-0.84
	CP	0.23/0.11	0.00/0.00	-8.44/-4.22	-8.44/-4.22	0.00	-1.23/-0.62				-0.81/-0.41
	EP	-3.77/-1.89		0.87/0.44	-27.06/-13.53	-1.07/-0.53	-7.31/-3.66	-0.4/-0.20	-2.44/-1.22	-3.19/-1.60	-4.97/-2.49
2014	WP	-12.30/-4.10		-40.61/-13.54	-2.77/-0.92	-17.99/-6.00	-21.86/-7.29	-11.81/-3.94	-10.50/-3.50	-5.82/-1.94	-2.81/-0.94
	CP	1.50/0.50	-3.40/-1.13	-4.85/-1.62	-4.85/-1.62	-13.63/-4.54	-35.04/-11.68				-7.00/-2.33
	EP	-14.13/-4.71		-8.06/-2.74	-0.98/-0.33	-1.82/-0.61	-31.42/-10.47	-12.63/-4.21	-8.56/-2.85	-8.18/-2.73	-5.90/-1.97

943

944 Table II. Supplementary material. Changes in area (m²) and accretion/erosion rates (m yr⁻¹) for
945 the western (W), central (C) and eastern (E) profile for each natural dune field from 1992 to 2014.

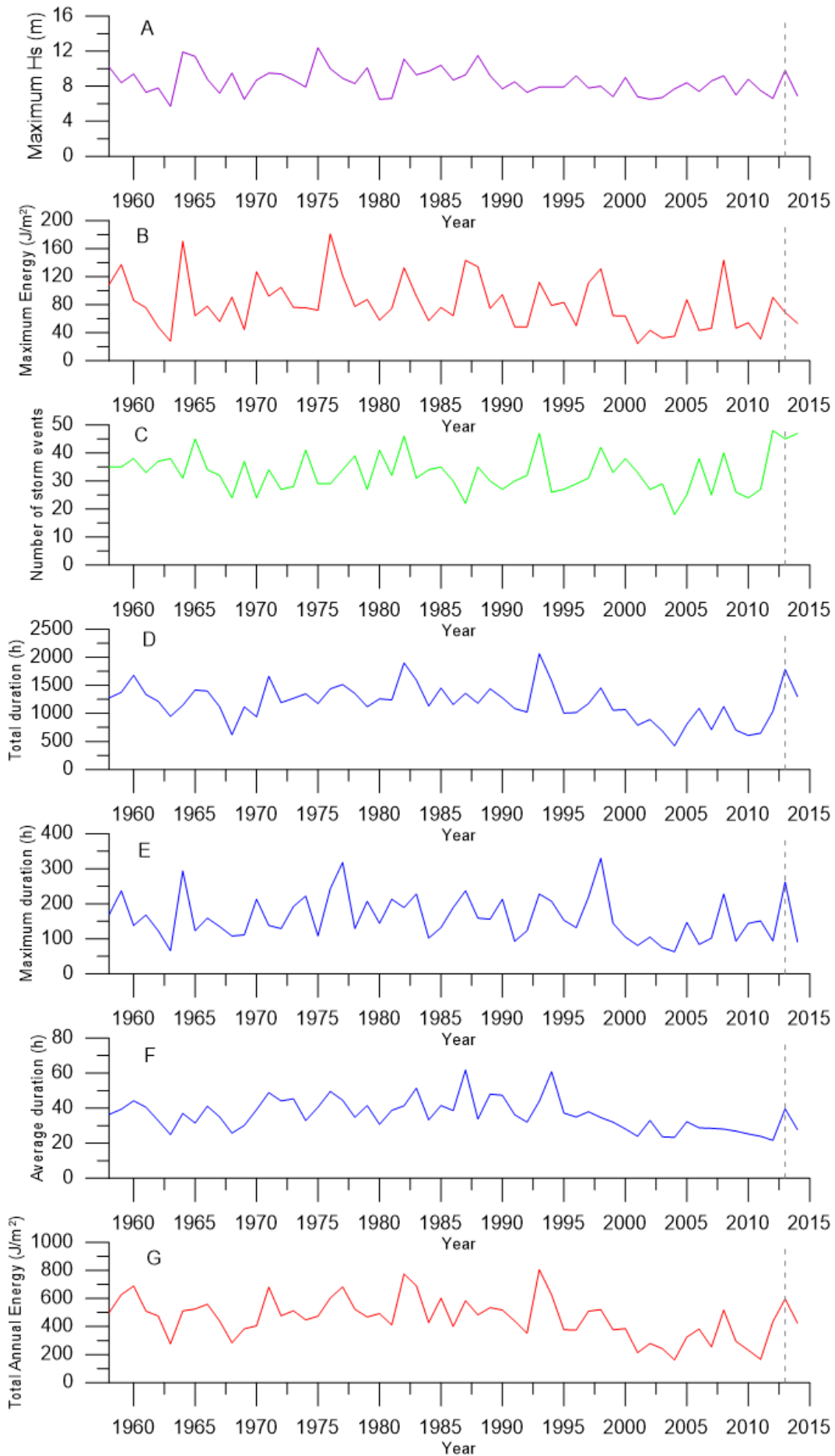
946



947

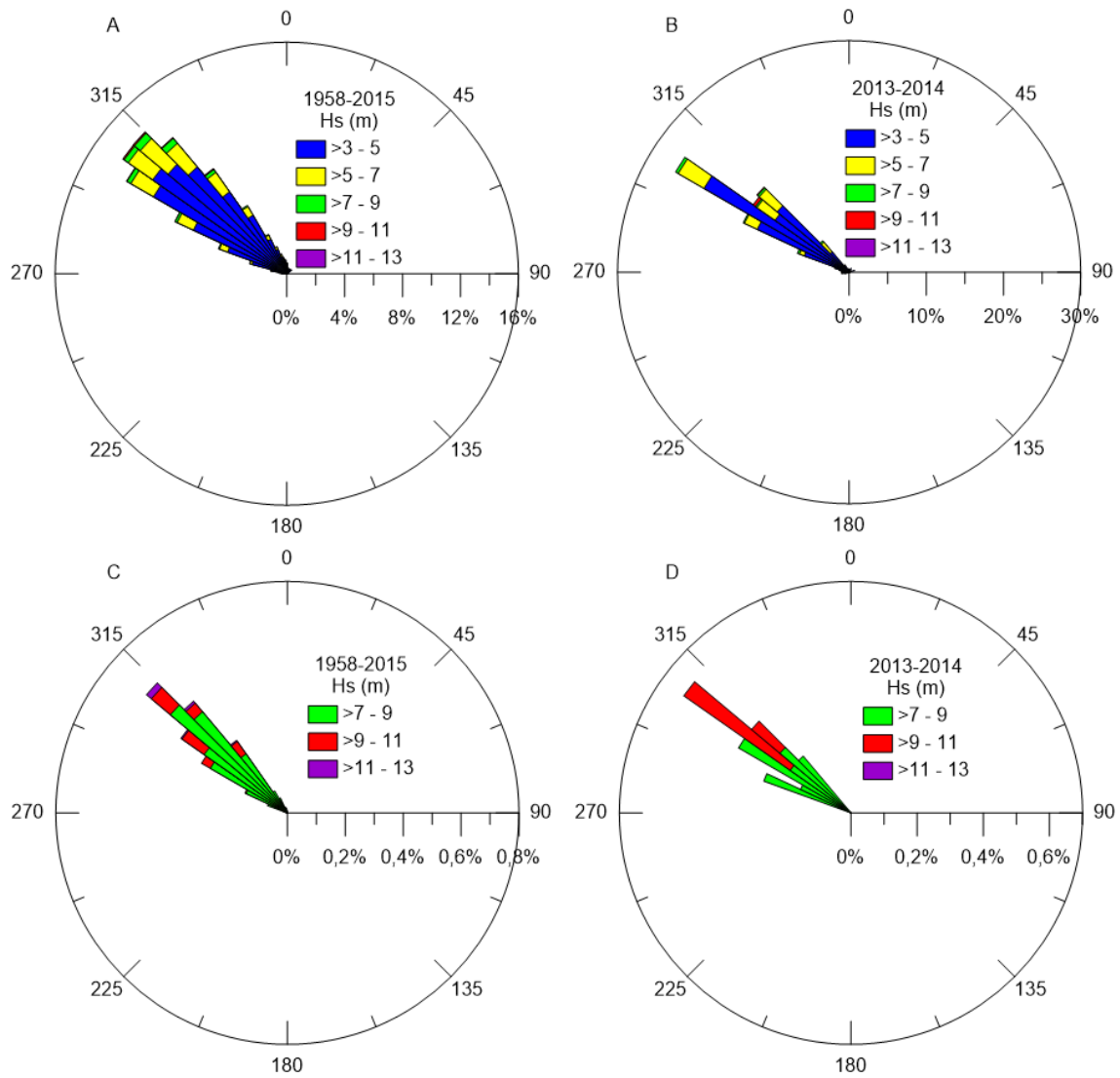
948 **Figure 2.** Location of the Asturian dune fields studied (black circles) and the riverine fluvial
 949 sources of sediments. 1) Peñarronda, 2) Mexota, 3) Sarello, 4) Navia, 5) Frejulfe, 6) Barayo, 7)
 950 Otur, 8) Quebrantos, 9) Salinas-El Espartal, 10) Xagó, 11) Carniciega, 12) Rodiles, 13) La Isla,
 951 14) Espasa, 15) Vega. Dune field removed (grey circle): Angueiro.

952



954 **Figure 2.** Statistics of storm events ($H_s > 3\text{m}$) for each climatic year from 1958-1959 to 2014-2015:
955 A) Maximum H_s ; B) Maximum energy of a storm event; C) Number of storm events; D) Total
956 duration for the whole of storm events; E) Maximum duration of a storm event; F) Average duration
957 of storm events; and G) Total annual energy. Data for each climatic year is plotted as
958 corresponding to its starting year (i.e. data for climatic year 2014-2015 are plotted as
959 corresponding to 2014). H_s is in m, duration in hours (h) and energy in $\times 10^6 \text{ J/m}^2$. The dashed line
960 indicates the climatic year 2013-2014.

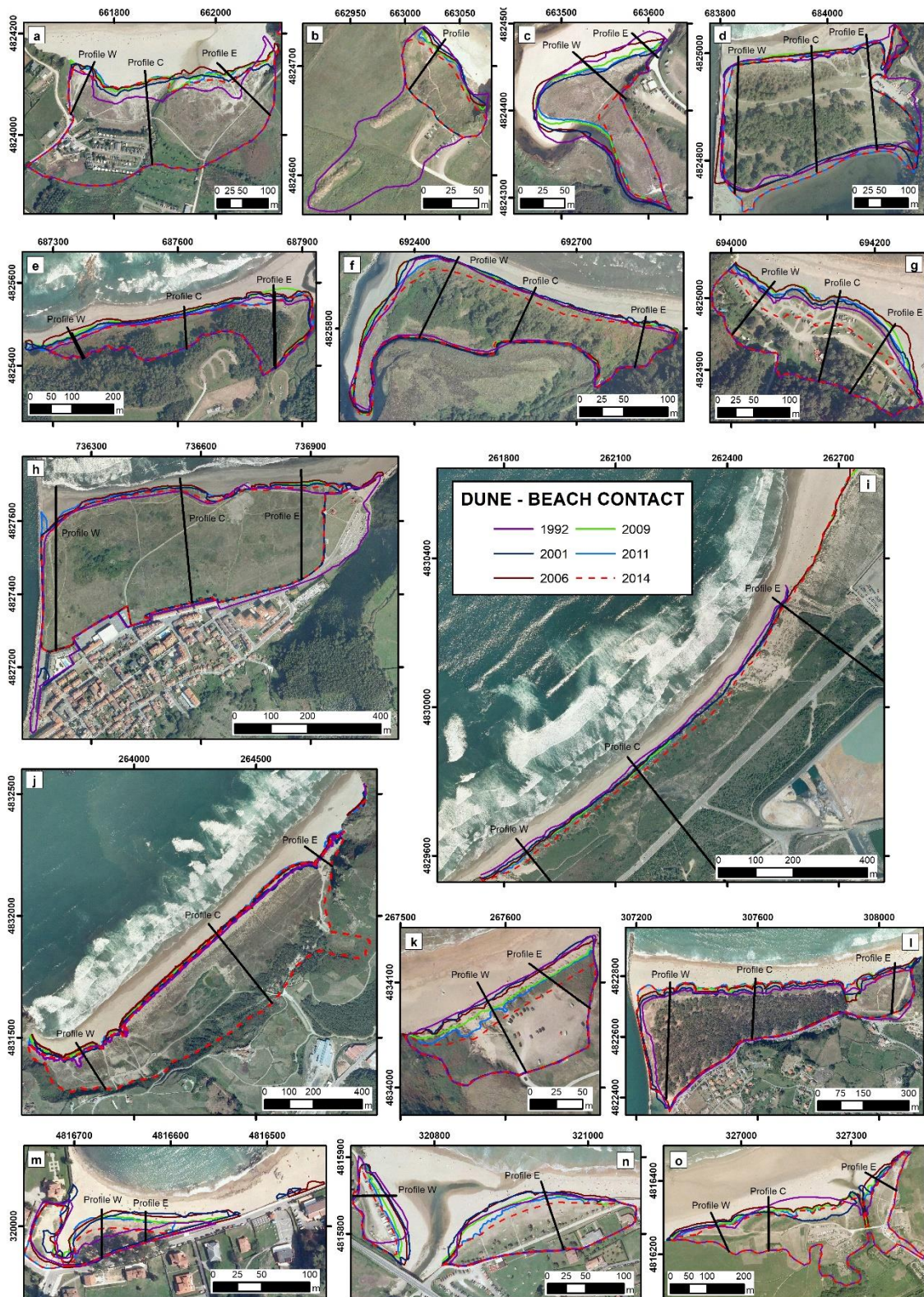
961



962

963 **Figure 3.** Directional histograms of storm waves ($H_s > 3$ m) for A) the 1958-2015 period, and B)
 964 the climatic year 2013-2014. Directional histograms of extreme storm waves ($H_s > 7$ m) for C) the
 965 1958-2015 period, and D) the climatic year 2013-2014.

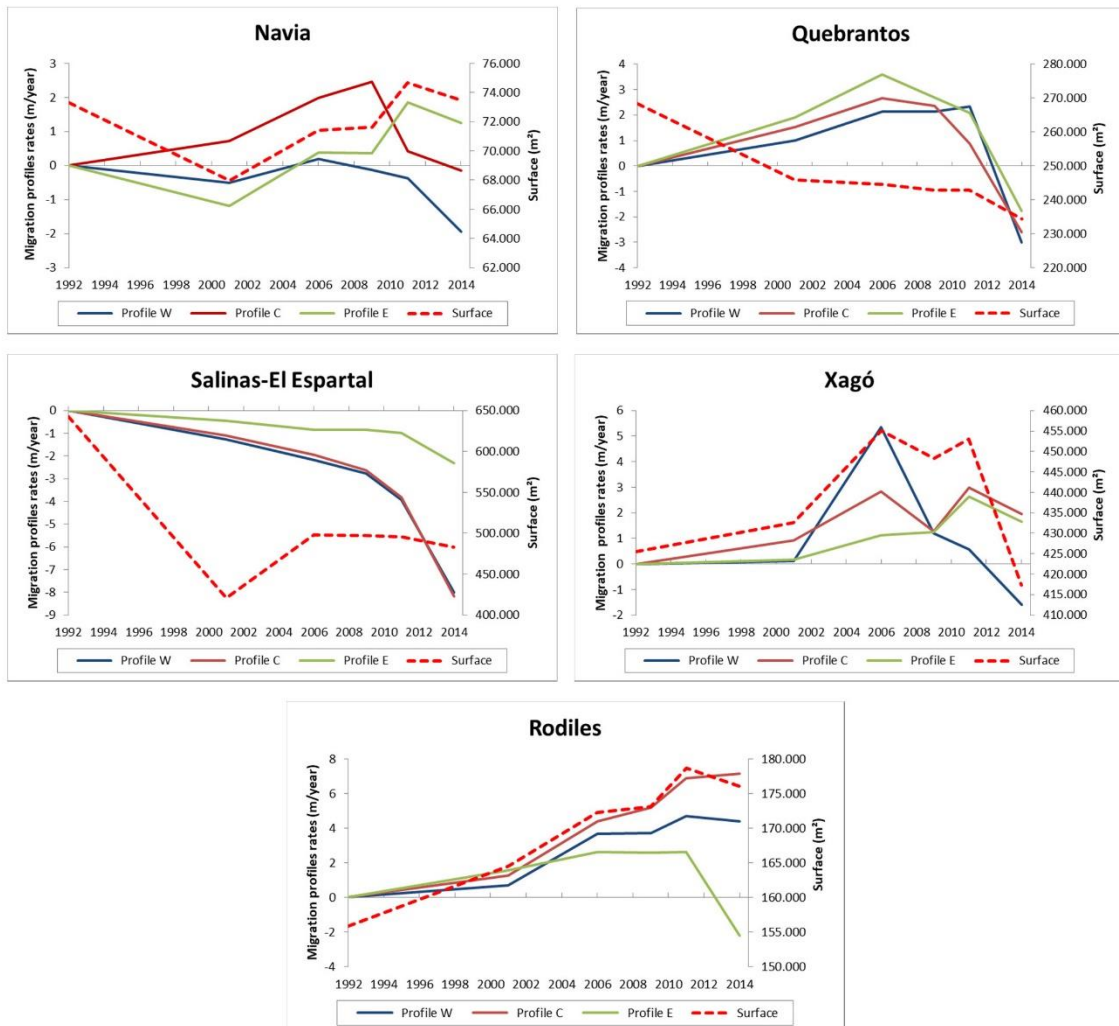
966



967

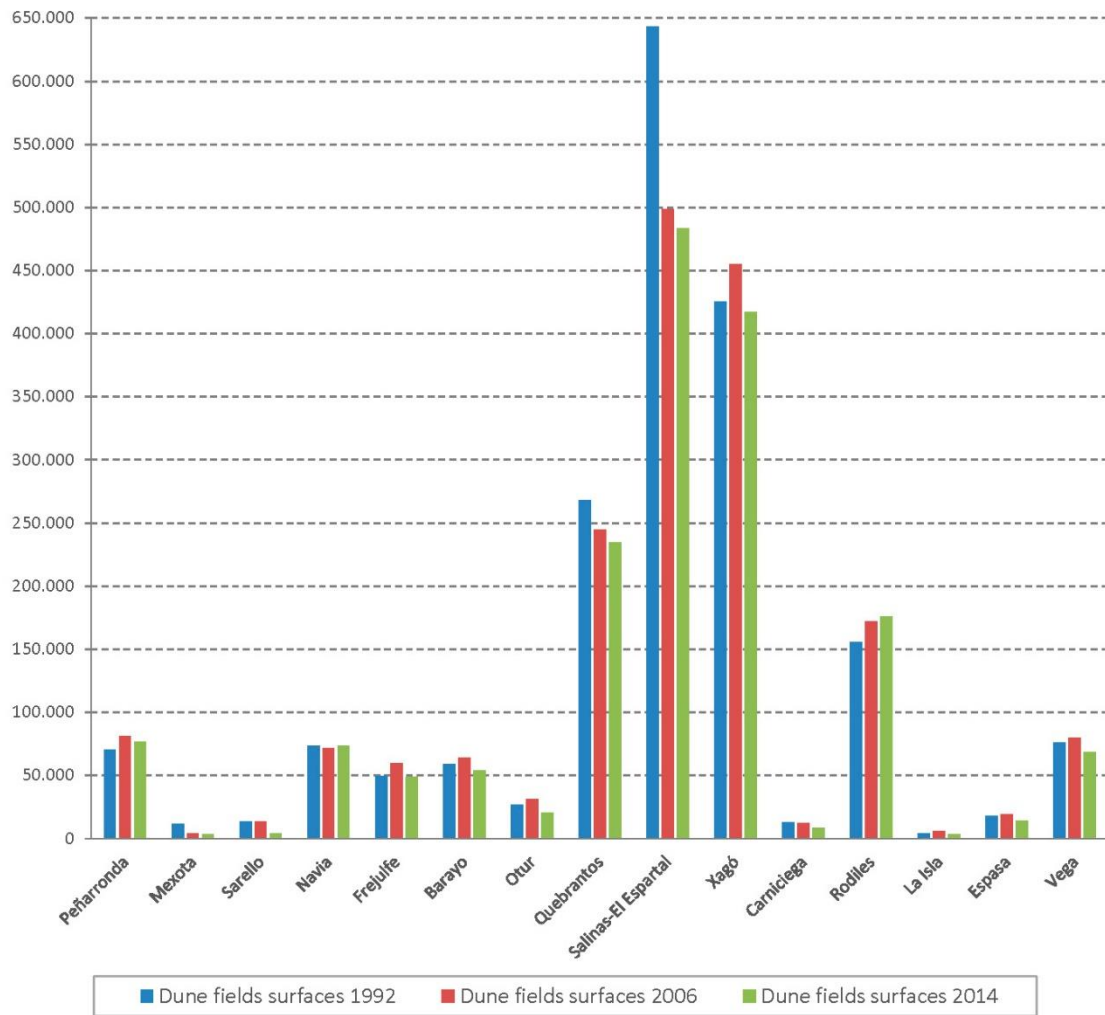
968 **Figure 4.** Evolution (1992-2014) of the beach-dune shoreline and location of measured profiles
 969 for each dune field. Orthophotographs are 2011. Dune coastlines include: a) Peñarronda, b)
 970 Mexota, c) Sarello, d) Navia, e) Frejulfe, f) Barayo, g) Otur, h) Quebrantos, i) Salinas-El Espartal,
 971 j) Xagó, k) Carniciega, l) Rodiles, m) La Isla, n) Espasa and o) Vega.

972
973
974



975
976
977
978
979

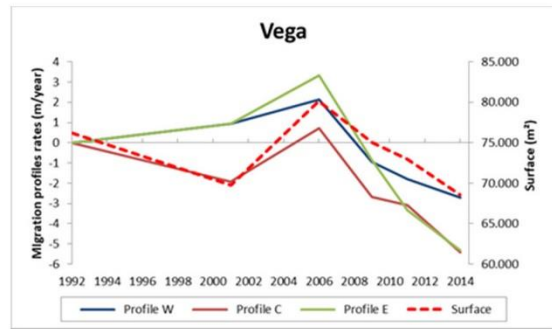
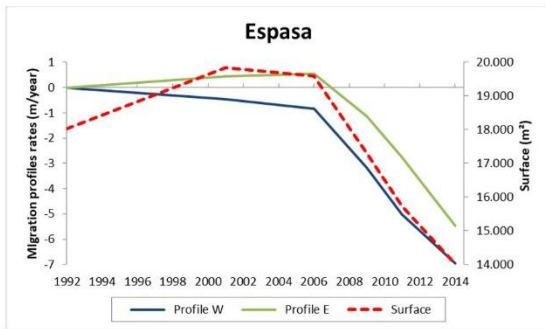
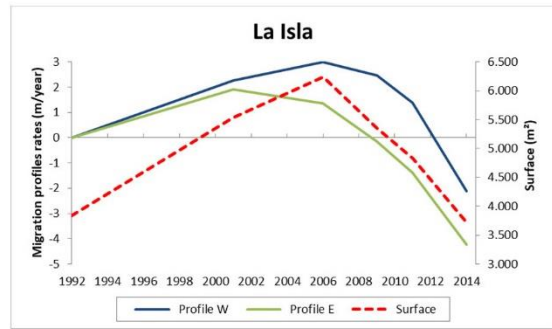
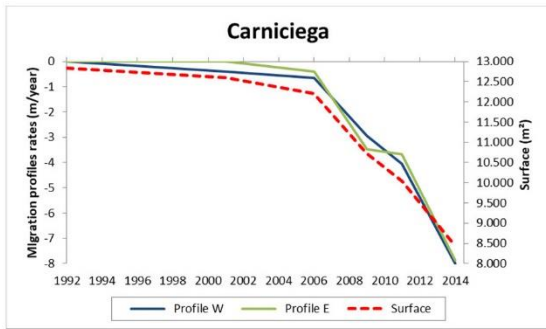
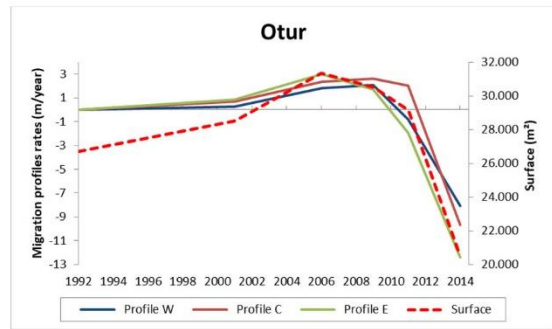
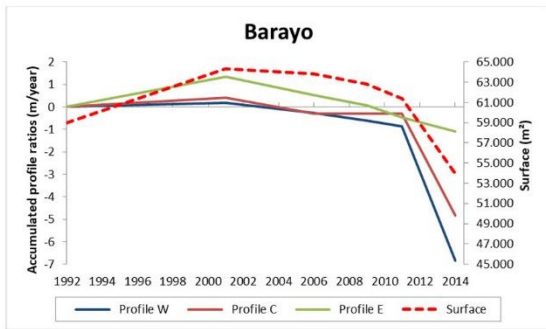
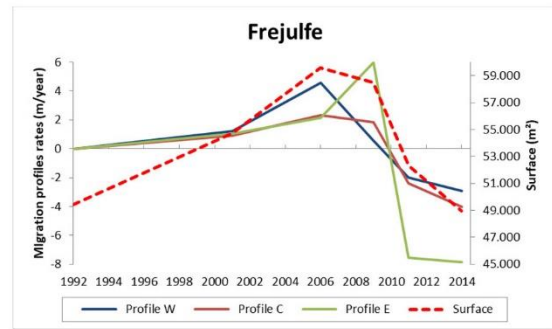
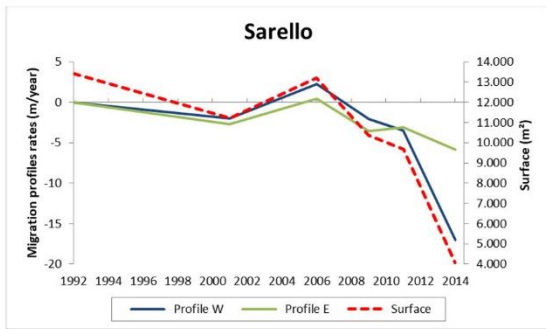
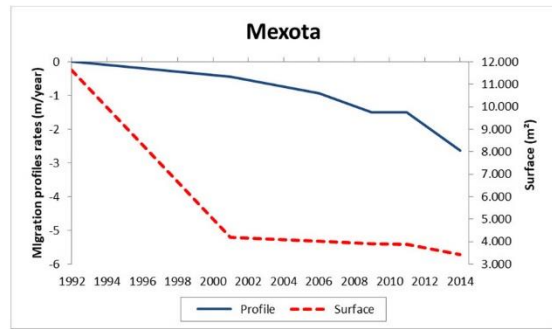
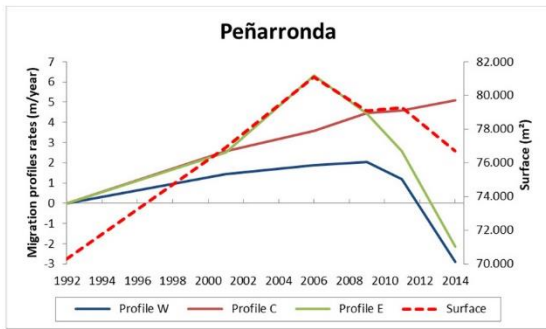
Figure 5. Shoreline evolution and surface area changes at human-impacted dune sites. The dashed red line represents changes in dune field area from 1992 until 2014. Accretion/erosion rates ($m\ yr^{-1}$) are shown for the three profiles established at each dune/beach system.



980

981 **Figure 6.** Surface variations (m²) of dune fields studied, comparing three representative
 982 moments: 1992 (blue), 2006 (red) and 2014 (green).

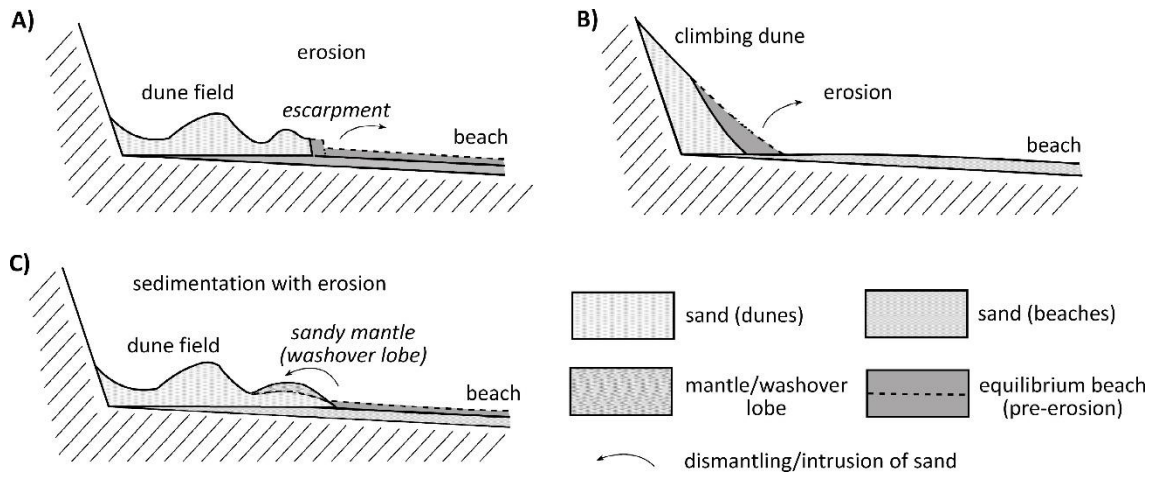
983



985 **Figure 7.** Shoreline evolution and surface area changes at natural sites. The dashed red line
986 represents changes in dune field area from 1992 until 2014. Accretion/erosion rates (m yr^{-1}) are
987 shown for the three profiles established at each dune/beach system.

988

989



990

991 **Figure 8.** Conceptual models of beach dunes response to 2013-2014 storm waves (without
 992 scale). Based in Hesp (2002).

993

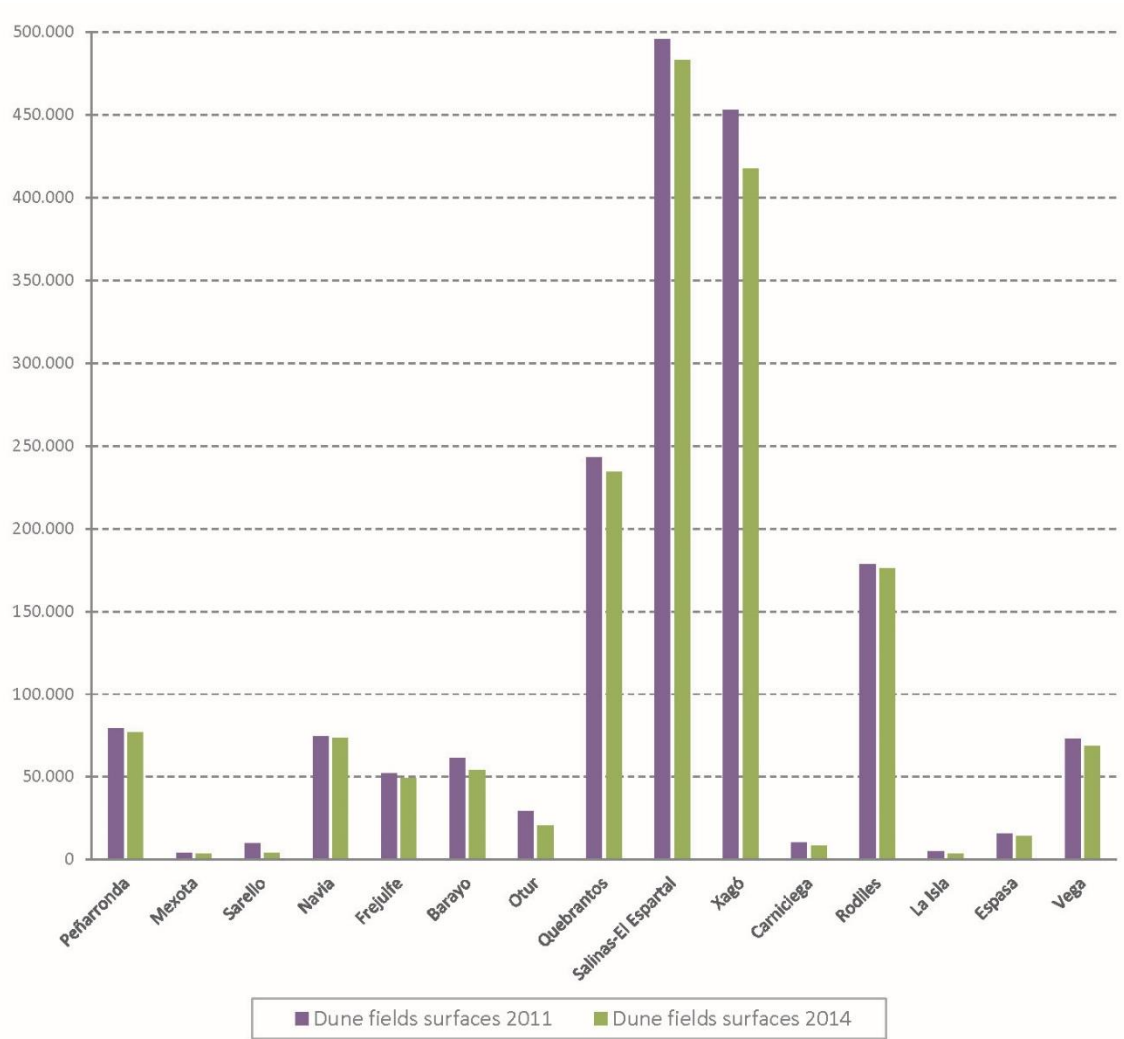


994

995 **Figure 9.** Photographs were taken on April of 2014 (west to east): A) Mexota. Climbing dune
 996 eroded since 70s, nowadays with a high slope, B) Navia, fore-dune confined by jetties. In 2014

997 some fan lobe covered the dune field, C) Barayo foredune lost until 18 m in 2014 surge storms,
998 D) Otur was the dune field more affected by 2014 wave storms (-35 m), E) East of Rodiles
999 foredune, with recession of 14.54 m in 2014, F) El Espartal retreated until 13 m since 2014,
1000 influenced by port management G) Carniciega climbing dune with a recession of 12.60 m in 2014,
1001 H) Vega foredune was one of the most damaged (-7 m). On the beach, a fallen milestone
1002 (demarcation line) of the terrestrial public domain (Spanish Coastal Law).

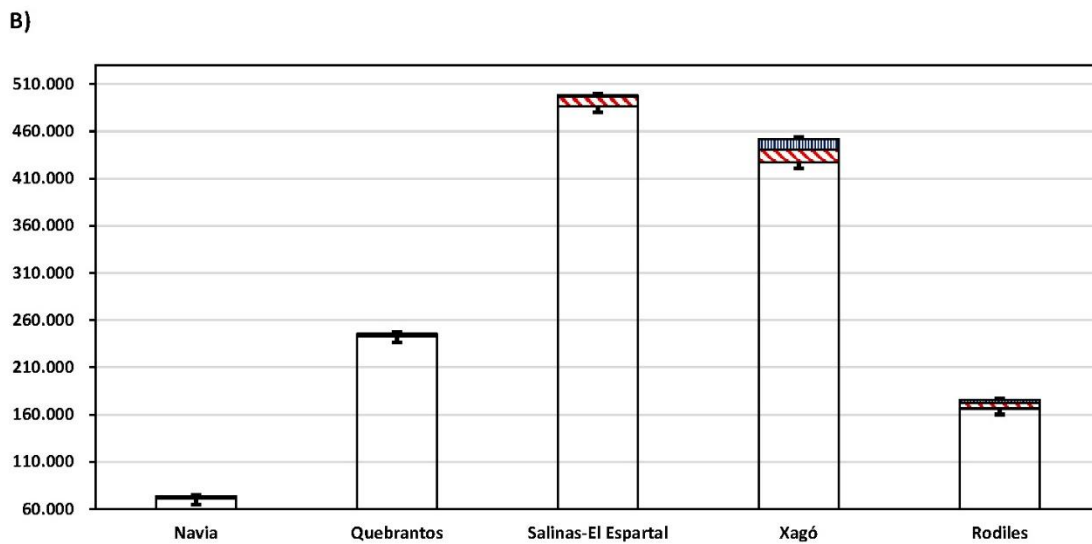
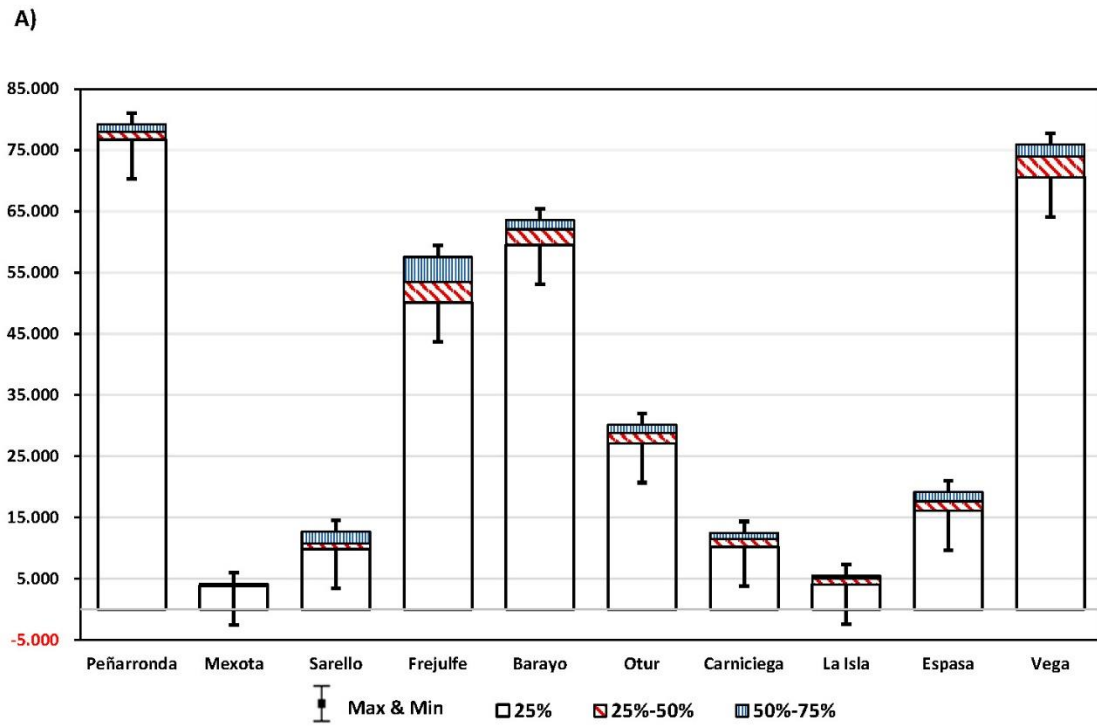
1003



1004

1005 **Figure 10.** Surface variations (m²) of dune fields studied after the greatest wave storms during
 1006 winter of 2014, comparing two periods: 2011 (purple), and 2014 (green).

1007



1008

1009 **Figure 11.** Statistics of surface averaged evolution during 1990's to 2014. A) Natural dunes, B)

1010 Anthropic-influenced dunes.

1011



1014 **Figure 12.** Photographs were taken during 2020 (west to east) showing shoreline recovery of
1015 sites shown previously in figure 9: A) Mexota. Increased sedimentary volume on the beach and
1016 attenuated recession, B) Navia, after continuous overflows in recent years, the dune has migrated
1017 landward (photograph provided by Efrén García Ordiales), C) Barayo. Dune intervened as part of
1018 the Life + Arcos project. re-profiling activities, D) Otur. Slope reduction (3 m high in 2014) and
1019 generation of a new foredune with pioneer vegetation at its base, E) East of Rodiles. Large sandy
1020 volumetric increase on the beach and generation of vegetated dunes at its base, F) El Espartal.
1021 Volumetric increase on the beach, less accelerated recession and dependent on dredging from
1022 Avilés estuary, G) Carniciega. Continued recession but with more sediment on the beach, slope
1023 decreased, H) Vega. Foredune recession stopped (Life + Arcos project) and dunes developing
1024 pioneer vegetation.

1025